COLLISION INDUCED FRAGMENTATION OF PYRENE CLUSTERS

Sébastien Zamith, Jean-Marc L'Hermite, Léo Dontot, Mathias Rapacioli, Fernand Spiegelman

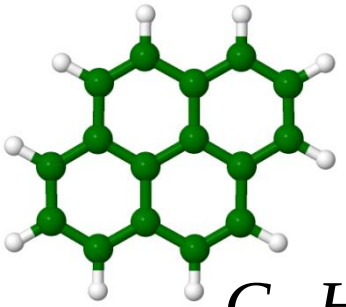

$C_{16}H_{10}$

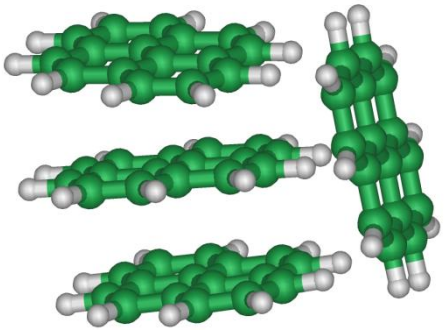

Université de Toulouse

cnrs dépasser les frontières

IRSAMC LCAR - LCPQ - LPCNO - LPT

Motivations

- Polycyclic aromatic hydrocarbons (PAHs) are present in soot
- Potentially in space

- PAH clusters: ‘natural’ form for soot, candidates for IR signature in space

Pyrene clusters

- Lowest energy structures calculated by combining DFTB and configuration interaction to deal with charge resonance (M. Rapacioli, L. Dontot and F. Spiegelman)

- Access to theoretical binding energies:

$E_0(n) = E(n) - E(n-1) - E(1)$

➔ This work: threshold CID experiments provide in principle access to dissociation energies

Threshold Collision Induced Dissociation

Fragmentation cross-section as a function of collision energy

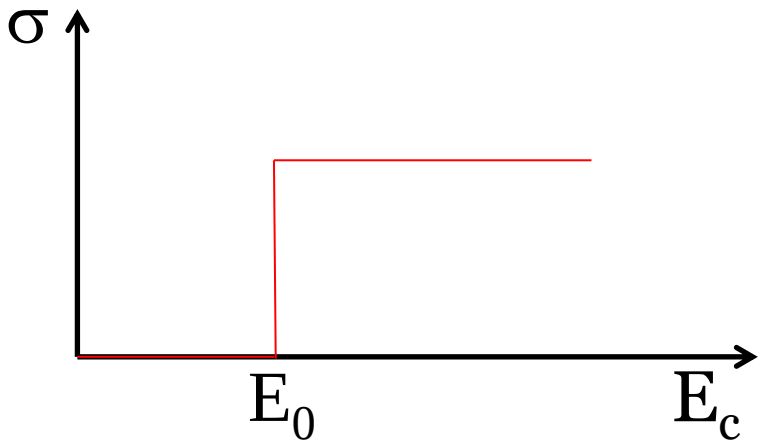

Idealized case:
Single collisions
Single collision energy
No initial internal energy
Total collision energy transfer in internal energy
If internal energy > E_o, fragmentation

In practice:
Multiple collisions
Distribution of collision energies
Partial collision energy transfer
Thermal initial internal energy
Statistical evaporation after energy deposition

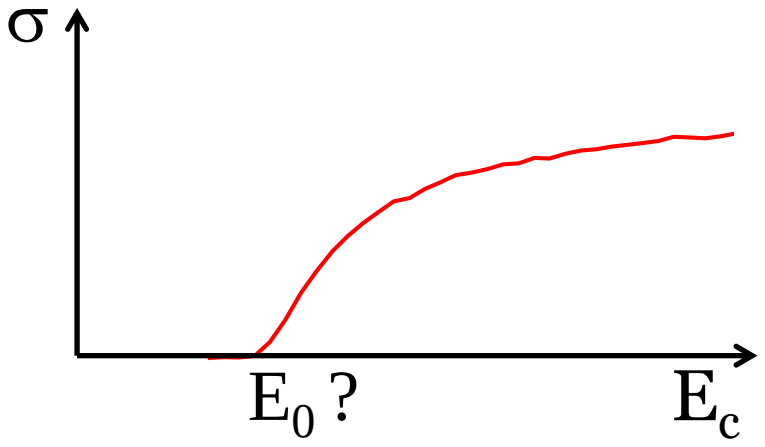

Outline

- Experimental setup
- Fragmentation cross-section determination
- Experimental fragmentation cross-sections *vs* E_c
- Fragmentation thresholds determination, comparison with theory
- Conclusion

Experimental setup

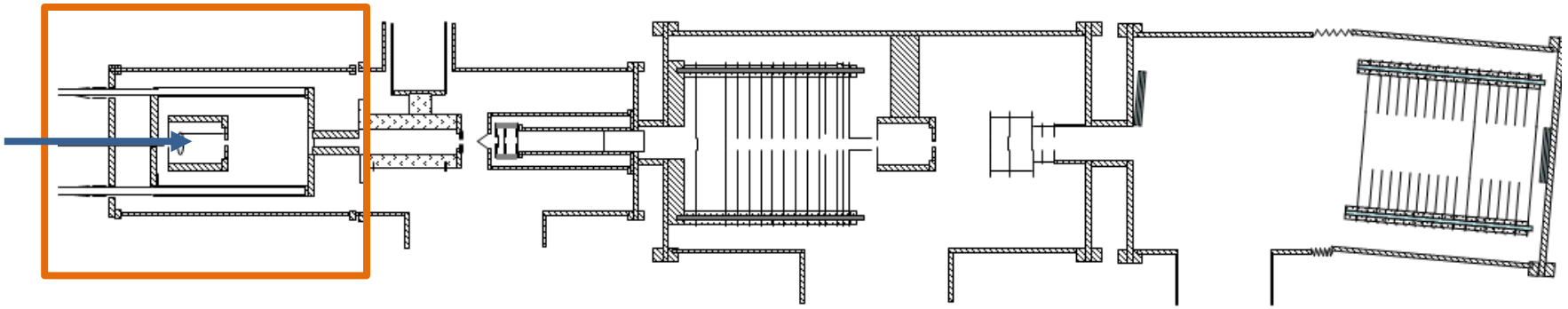

- Gaz aggregation source, n = 1-40

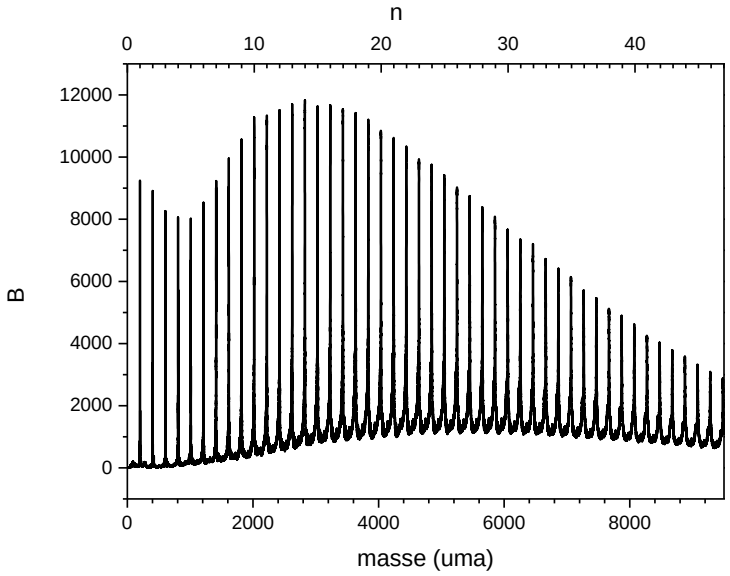

$(Py)_n^+$

Experimental setup

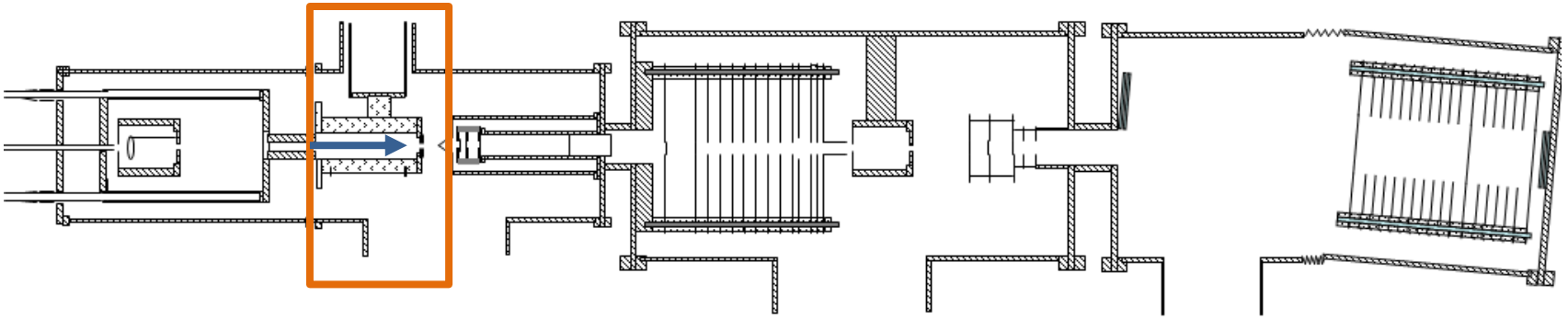

- Thermalization : T = 25 K

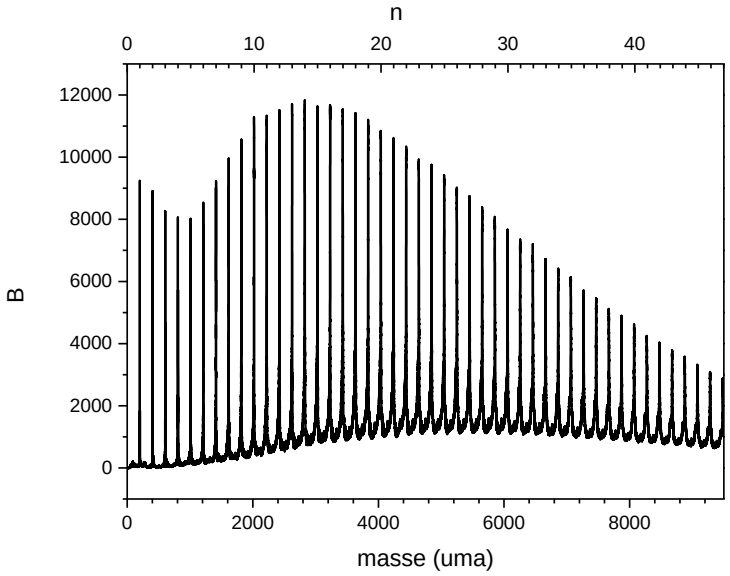

canonical distribution
of internal energies E_i

Experimental setup

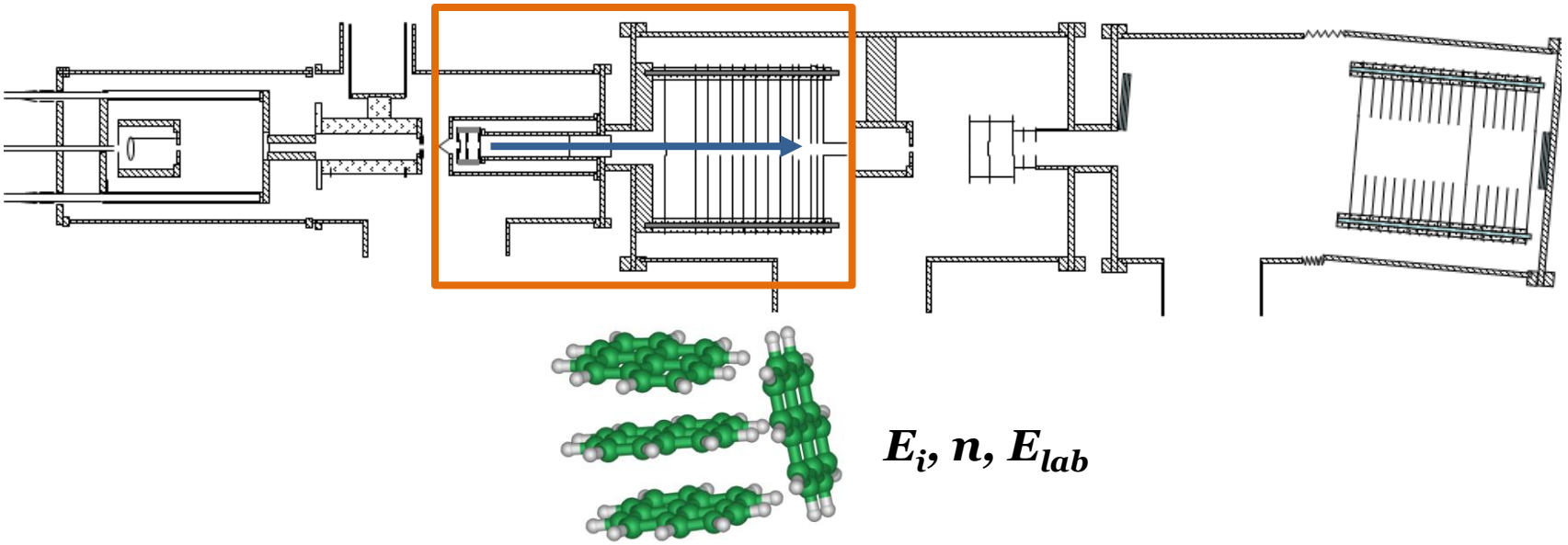

E_i, n, E_{lab}

- Mass selection, energy focussing, slowing down :
  E_{lab} = 5-400 eV

Internal energy E_i, microcanonical evolution

Experimental setup

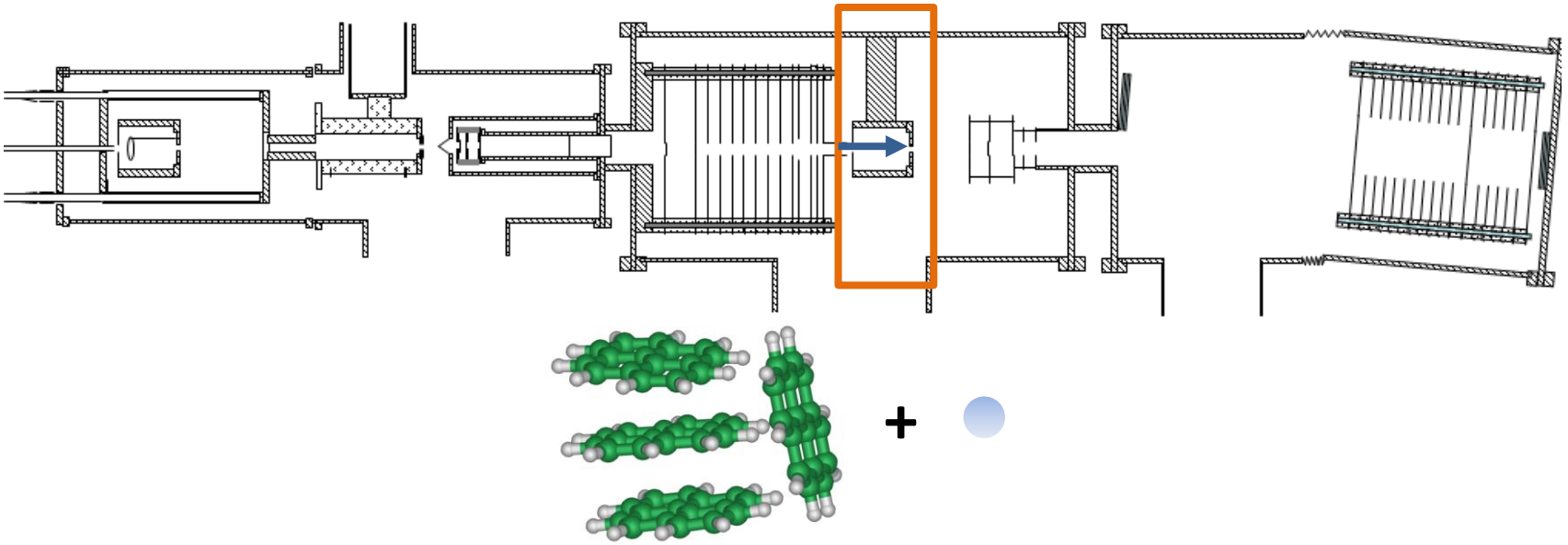

$$E_{cm} = E_{lab}\frac{m}{m+M} + \frac{3}{2}k_B T_{cel}\frac{M}{m+M}$$

- Collision with atoms (Ar), controlled pressure

Experimental setup

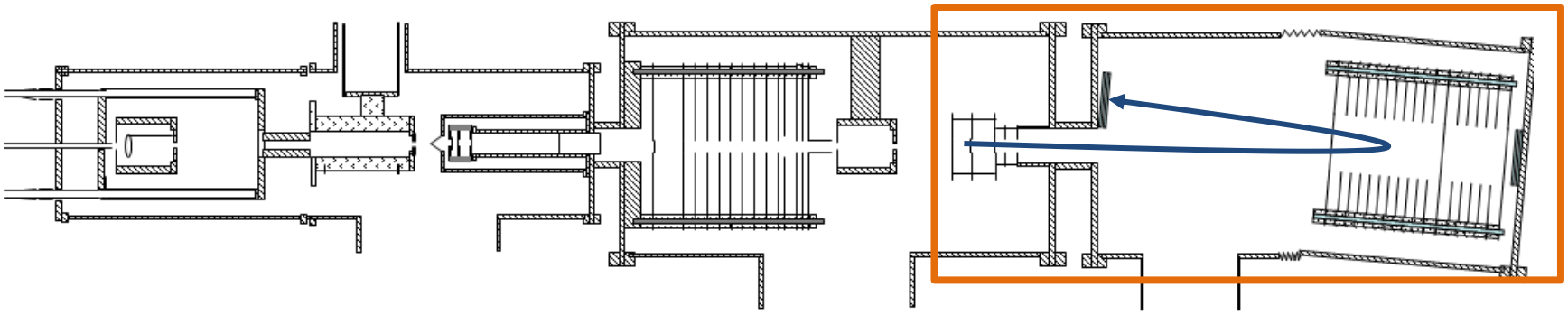

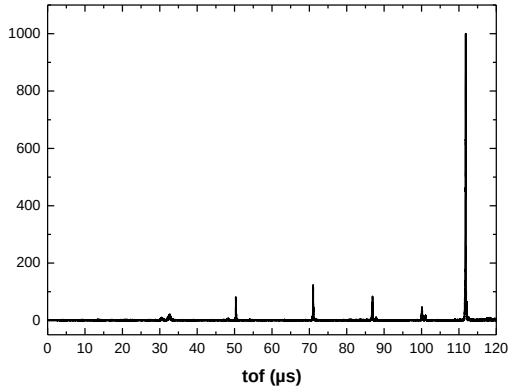

- Reaction products analyzed by TOF mass spectrometry

TOF mass spectrum

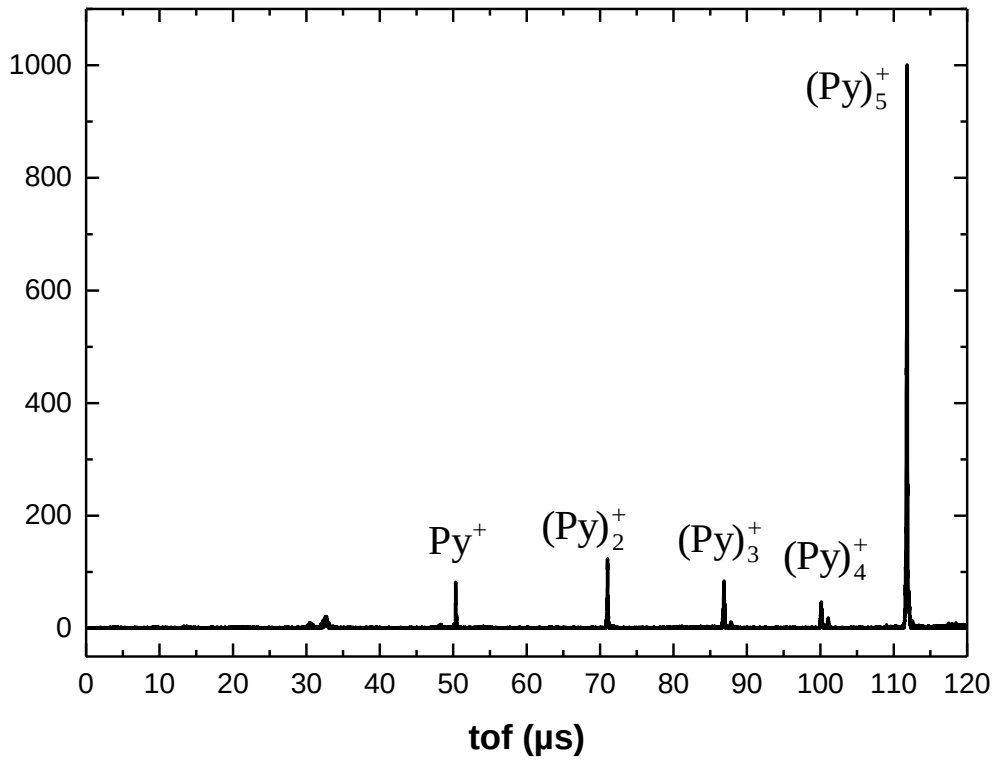

Argon pressure kept as low as possible to ensure single collision regime.

$(Py)_5$ cation colliding with Argon at 7 eV center of mass collision energy.

Fragmentation cross-section

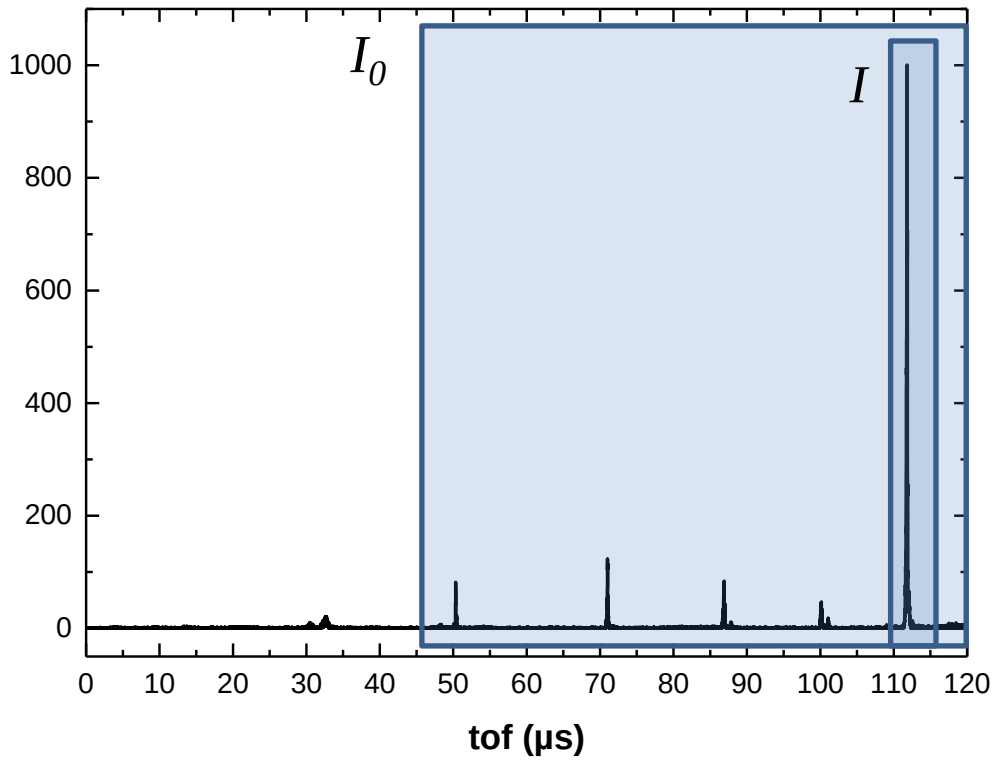

$$\sigma_{frag} = -\frac{\ln(I / I_0)}{\rho L_{cel}}$$

ρ = atomic density in the collision cell

L_{cel} = length of the collision cell

$(Py)_5$ cation colliding with Argon at 7 eV center of mass collision energy.

Fragmentation cross-section

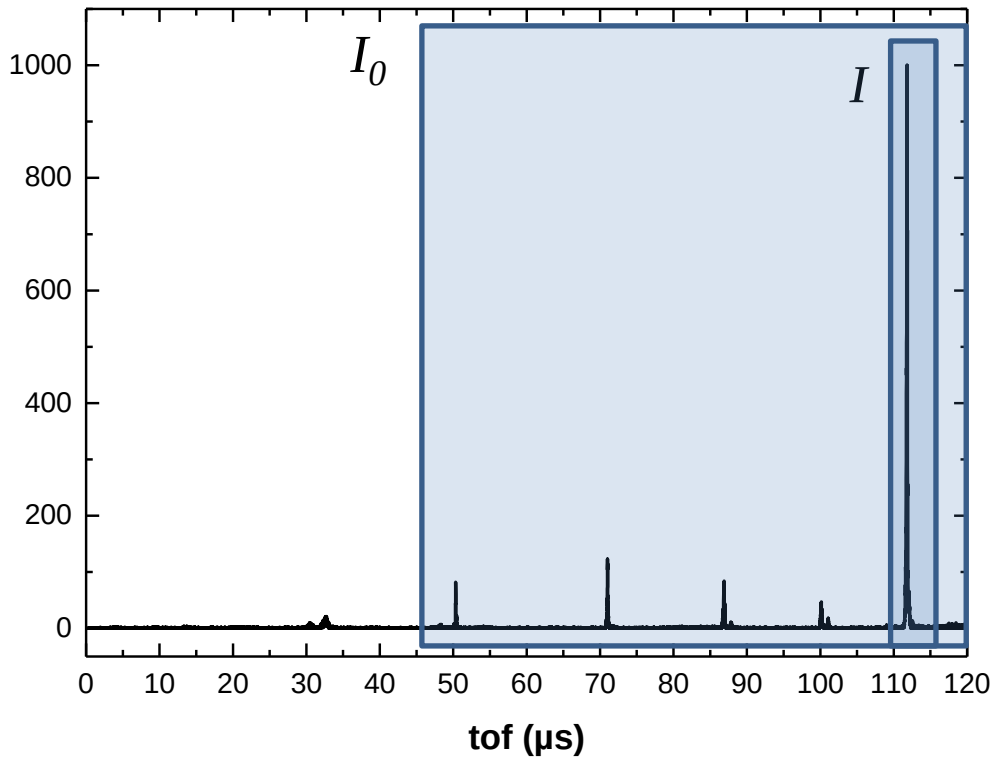

$$\sigma_i = BR_i \sigma_{frag}$$

BR_i = branching ratio for fragment of size i

$$BR_i = \frac{I_i}{\sum_i I_i}$$

$(Py)_5$ cation colliding with Argon at 7 eV center of mass collision energy.

Experimental results

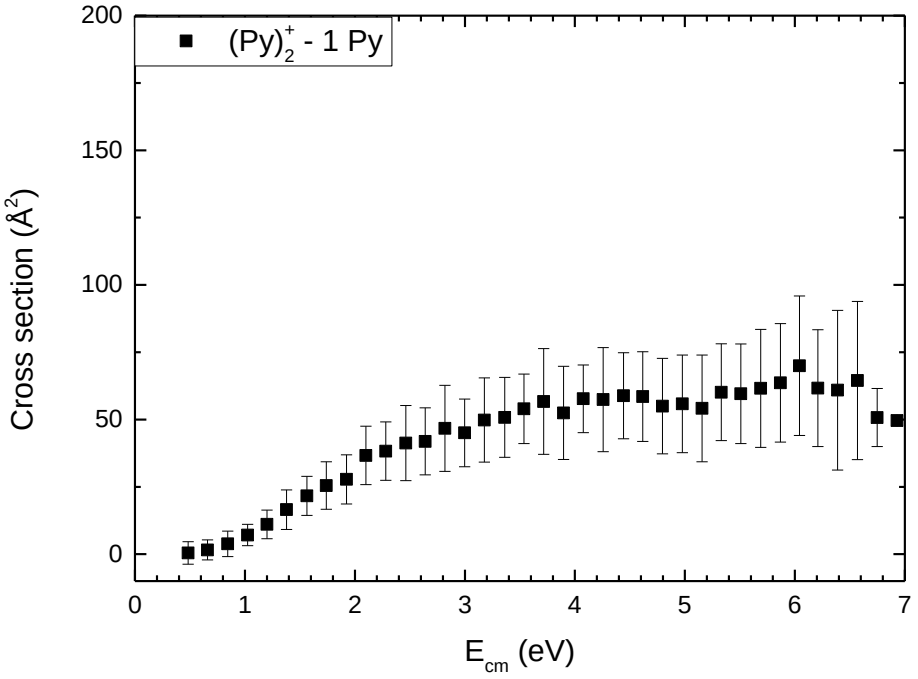

$(Py)_2^+ + Ar$

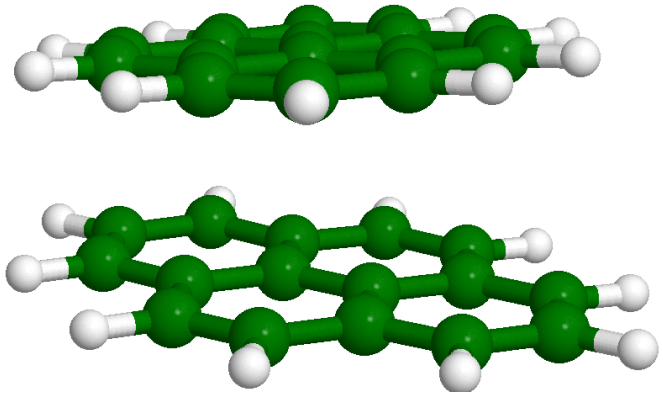

Calculated structure

(M. Rapacioli, L. Dontot and F. Spiegelman)

Theoretical fragmentation cross-section

Initial conditions:

Canonical distribution of internal energies at 25 K.
Clusters of size n, internal energies E_i.

Collision, energy transfer:

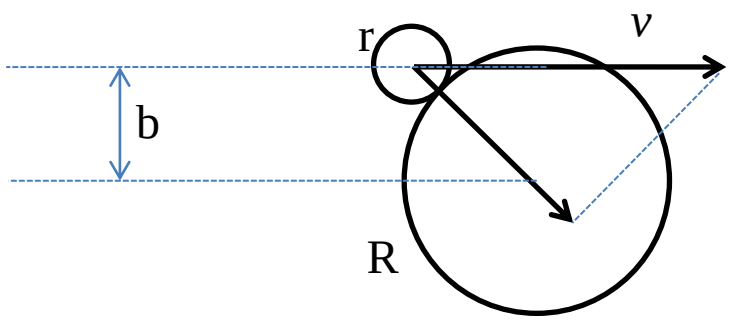

σ: geometric cross section $\pi(R+r)^2$
v : distribution of relative velocity
Collision rate : $\rho\sigma v$

After collision $E_i \rightarrow E_i' = E_i + 1/2\mu v^2(1 - b^2/(R+r)^2)$

Hypothesis: only radial part of the collision energy transferred.

Theoretical fragmentation cross-section

Statistical evaporation model (PST): $W(E) = \frac{G(E_f)}{hN(E_i')(2J+1)}$

Ingredients:
- density of states of the parent $N(E_i')$
- total number of states of the fragments $G(E_f)$
- conservation of total angular momentum J
- $E_f = E_i' + E_{rot} - E_0$

Approximations:
- harmonic vibrational frequencies from DFTB-CI
- all species considered as spherical tops
- ion-polar interaction between the neutral fragment and the charged cluster

Theoretical fragmentation cross-section

Evolution of the parent population across the collision cell:

$$\begin{cases} \dfrac{dI_n(E_i)}{dt} = -\rho\sigma < v > I_n(E_i) \\ \dfrac{dI_n(E_i')}{dt} = \rho\sigma v I_n(E_i) - W(E_i')I_n(E_i') \end{cases} \Rightarrow \begin{cases} I_n(E_i) = I_{n0}(E_i)e^{-\rho\sigma<v>t} \\ I_n(E_i') = \rho\sigma v I_{n0}(E_i)\dfrac{e^{-W(E_i')t} - e^{-\rho\sigma<v>t}}{\rho\sigma < v > -W(E_i')} \end{cases}$$

$$I_0 = \sum_{E_i} I_{n0}(E_i)$$

$$I = \sum_{E_i} I_n(E_i) + \sum_{E_i}\sum_{E_i'} I_n(E_i') \qquad \sigma_{frag} = -\frac{\ln(I/I_0)}{\rho L_{cel}}$$

- Propagation times taken into account
- Only first fragmentation considered, *i.e.* loss of a single Pyrene molecules (ok for Pyrene dimer).

Experimental results

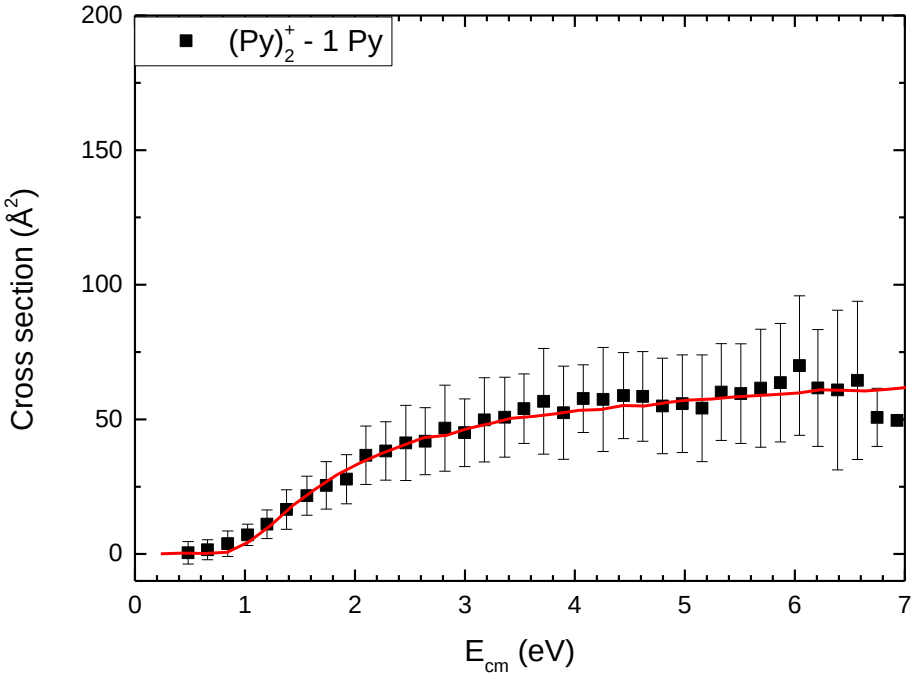

$(Py)_2^+ + Ar$

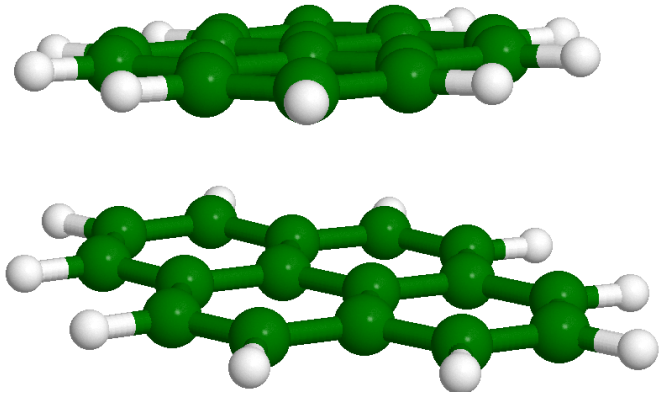

Calculated structure

(M. Rapacioli, L. Dontot and F. Spiegelman)

$E_0 = 1.0$ eV

Experimental results

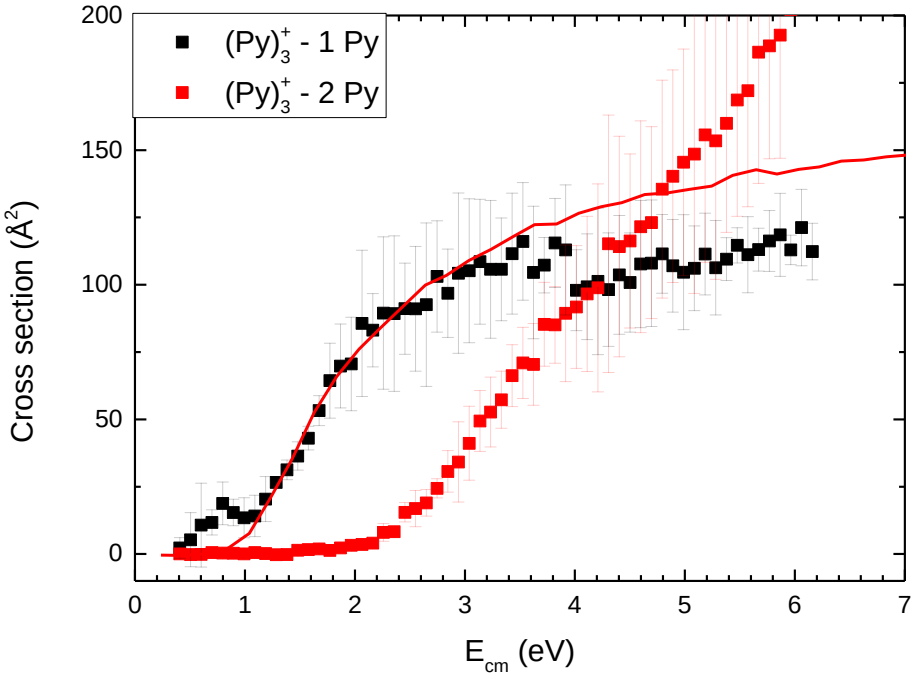

$(Py)_3^+ + Ar$

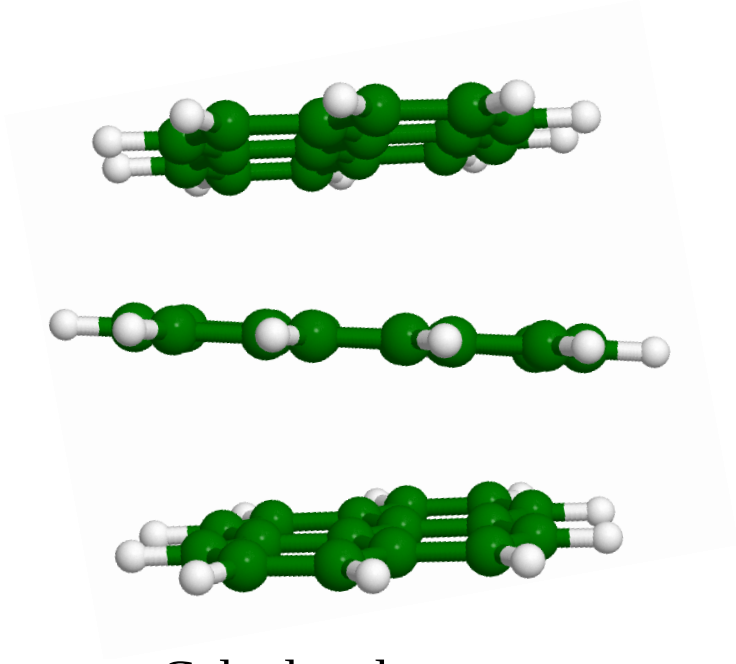

Calculated structure

(M. Rapacioli, L. Dontot and F. Spiegelman)

$E_0 = 0.8$ eV

Experimental results

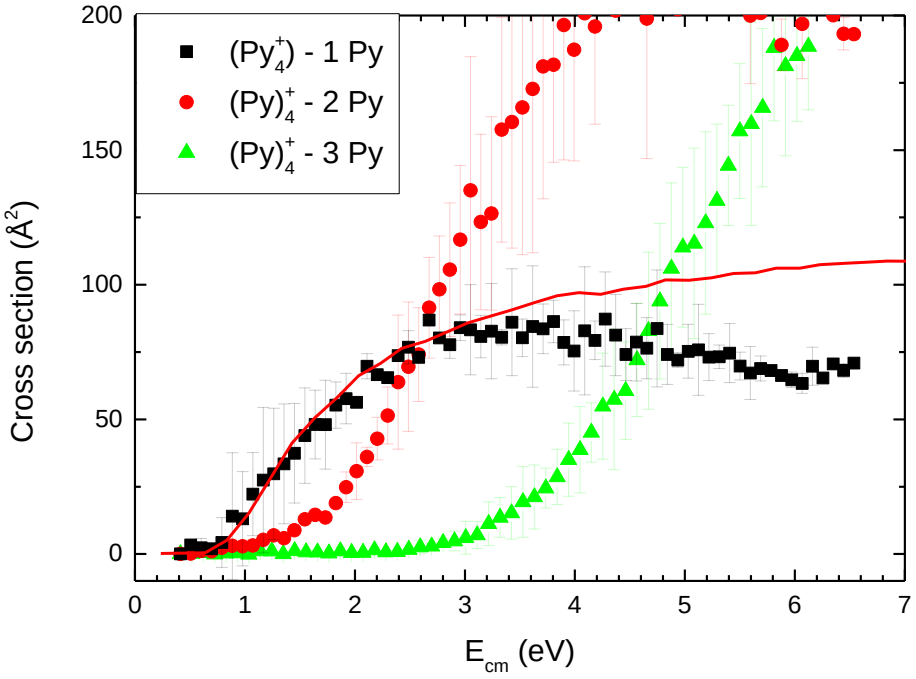

$(Py)_4^+ + Ar$

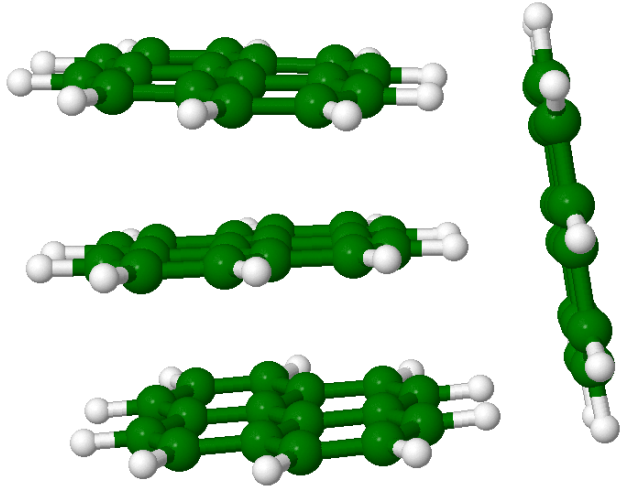

Calculated structure

(M. Rapacioli, L. Dontot and F. Spiegelman)

$E_0 = 0.7$ eV

First dissociation energies

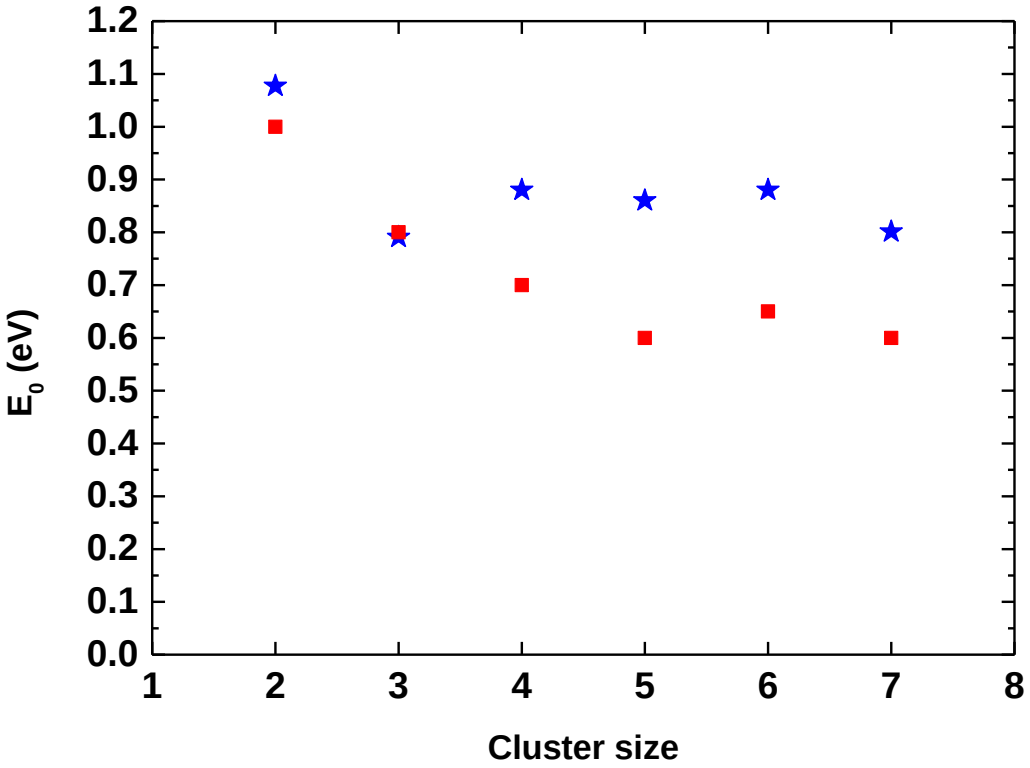

Blue stars: theory
Red squares: experiment

Limitations:

-Theoretical values determined as the difference between lowest energy structures

- Experimentally determined dissociation energies do not take into account successive evaporations

- Collision energy transfer efficiency?

- Statistical fragmentation?

Conclusions

-Fragmentation cross-section as a function of collision energy

- Experimental curves show threshold energies for sequential dissociations

- In practice, to relate these thresholds to dissociation energies, one needs:
  Knowledge of the energy transfer during collision
  Evaporation rates

- Independent measurement of evaporation rate *vs* initial temperature: validation of the calculated PST rate, coll. C. Joblin.

- Treatment of sequential evaporations by PST: reproduction of branching ratios

- For n>3, isomers?

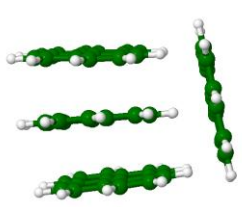

E_0 = 0.88 eV

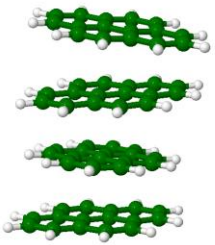

E_0 = 0.67 eV

Perspectives

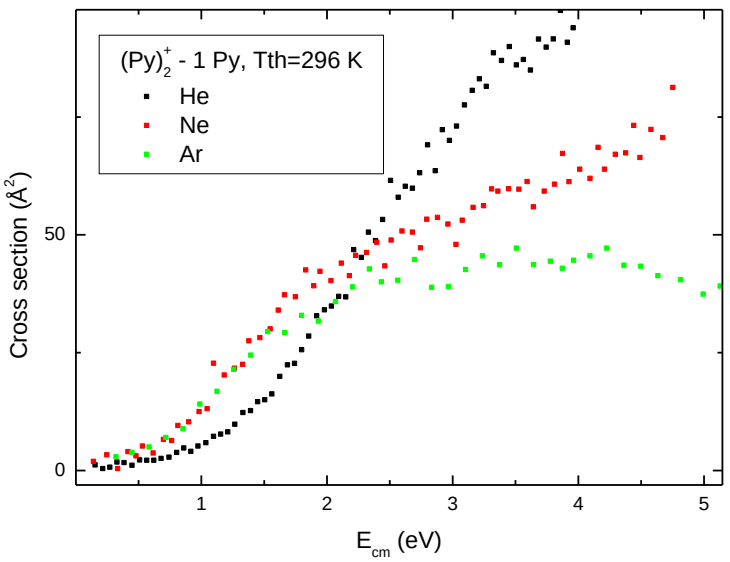

-Collision energy transfer:
Different collision gases have been used to fragment Pyrene dimer.
Ar and Ne show similar behaviors.
Inefficient collision energy transfer for He?

Simulations of collisions of rare gases with Pyrene clusters to evaluate the collisional energy transfer

Perspectives

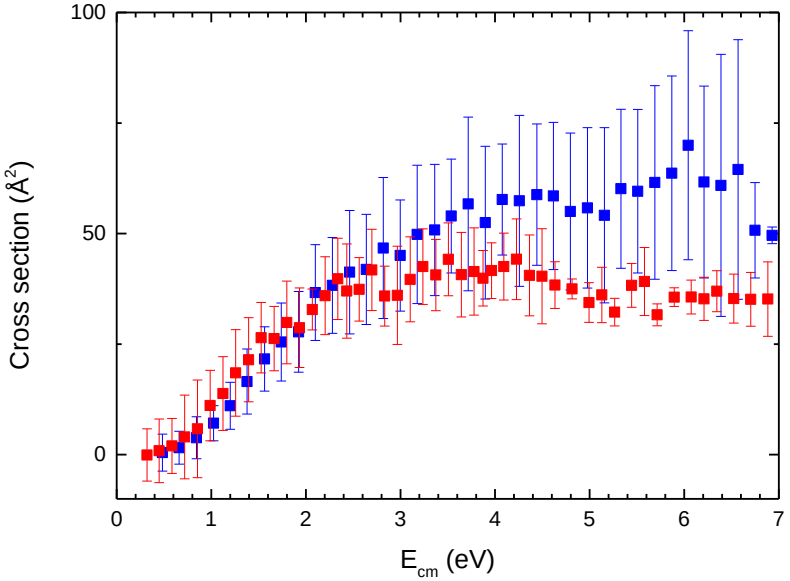

- Initial temperature effect on the fragmentation cross section: almost the same result at 25 and 300 K.
Very likely due to evaporation prior to collisions.
Intermediates temperatures will be studied.

- Study of heterogeneous clusters $(H_2O)_n(Py)_m$:

Attachment cross-section
Fragmentation cross-section
Nanocalorimetry

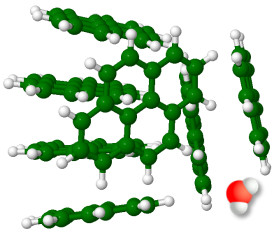

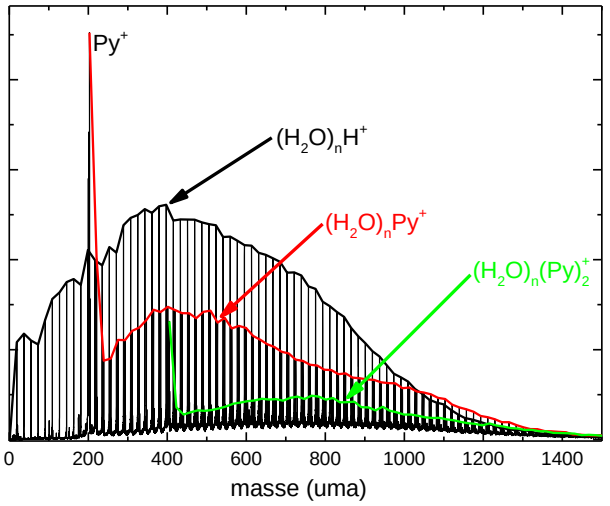

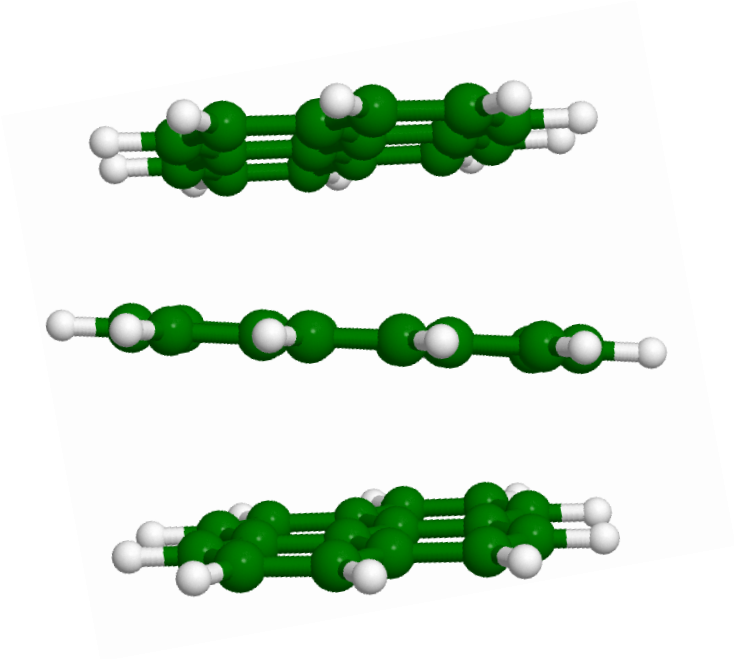

Calculated structure

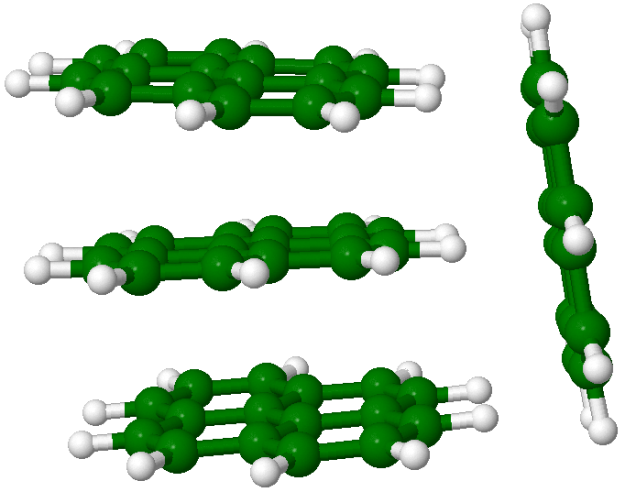

Calculated structure

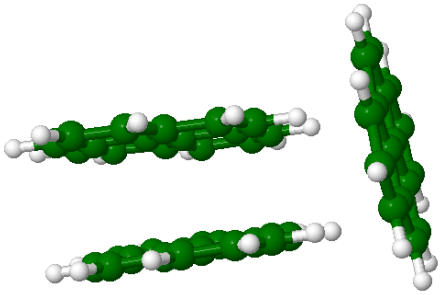

60 meV higher

k_BT@25K = 2 meV

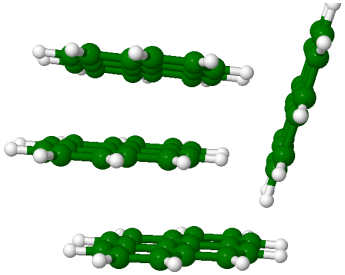

100 meV higher

k_BT@25K = 2 meV

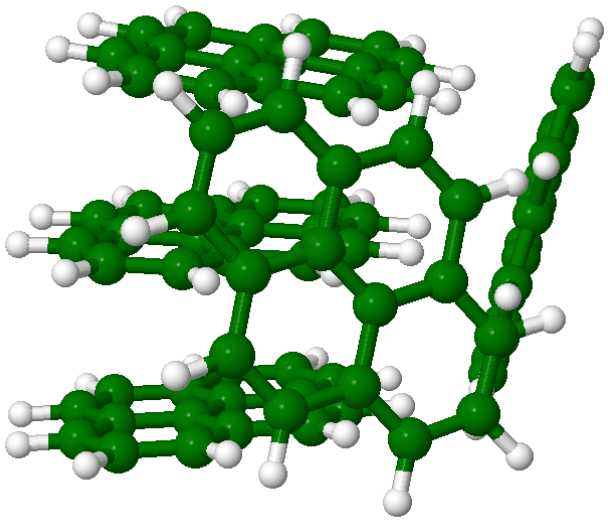

Calculated structure

(M. Rapacioli, L. Dontot and F. Spiegelman)

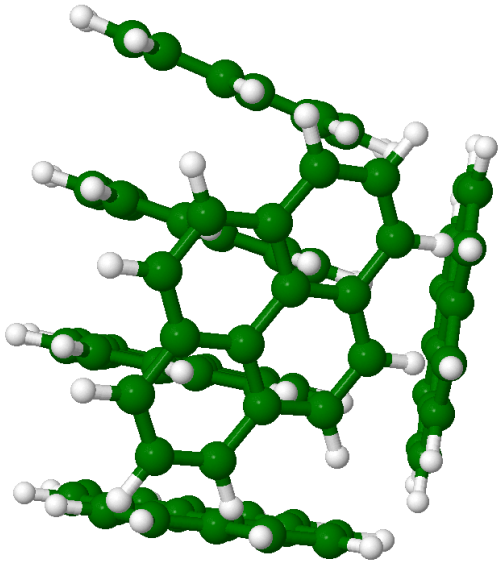

Calculated structure

(M. Rapacioli, L. Dontot and F. Spiegelman)

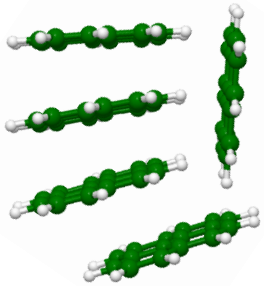

45 meV higher

k_BT@25K = 2 meV

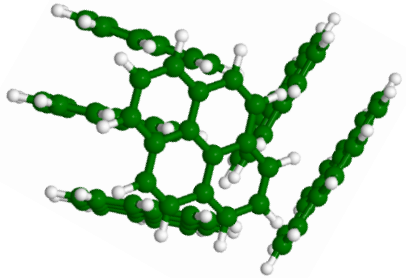

110 meV higher

k_BT@25K = 2 meV

Experimental results

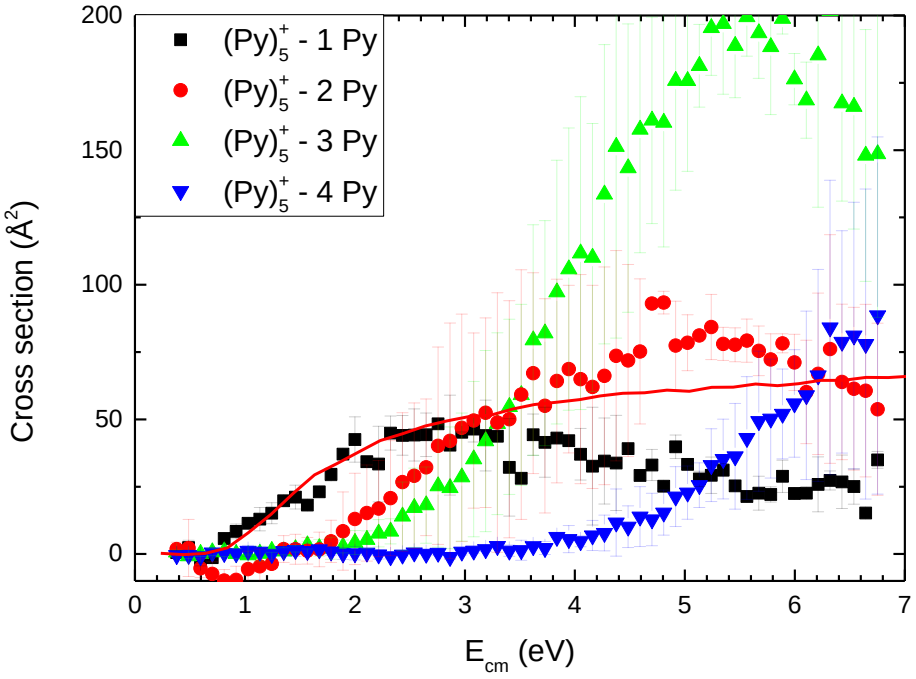

$(Py)_5^+ + Ar$

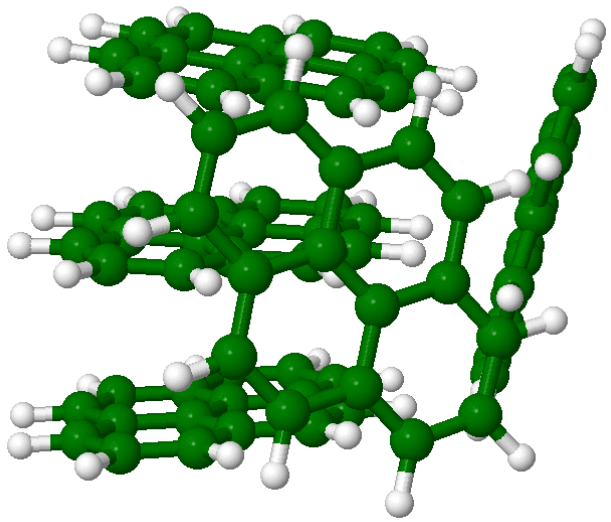

Calculated structure

(M. Rapacioli, L. Dontot and F. Spiegelman)

$E_0 = 0.60$ eV

Experimental results

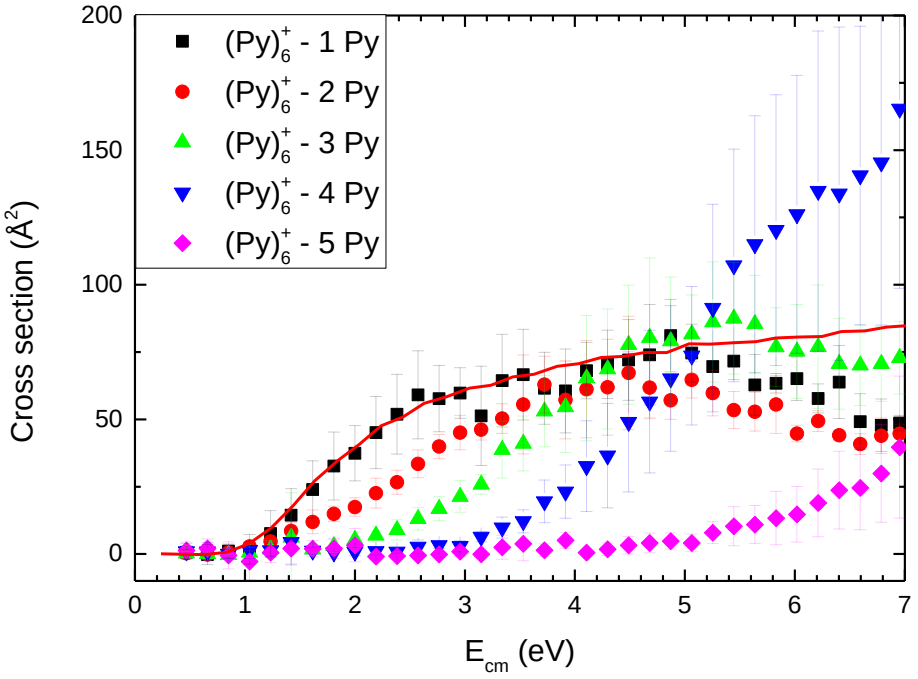

$(Py)_6^+ + Ar$

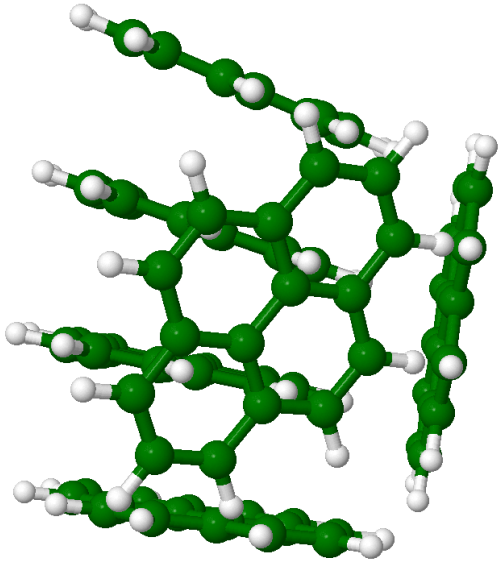

Calculated structure

(M. Rapacioli, L. Dontot and F. Spiegelman)

$E_0 = 0.65$ eV

Experimental results

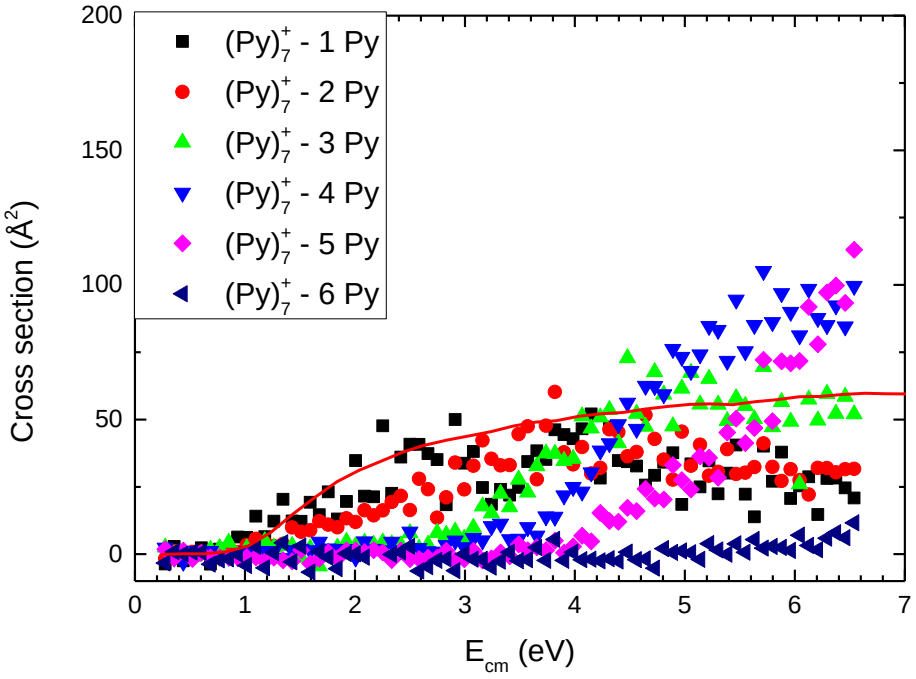

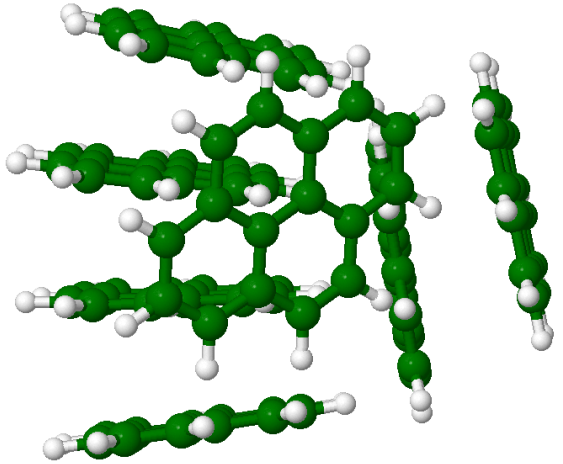

$(Py)_7^+ + Ar$

$E_0 = 0.60$ eV

Theoretical fragmentation cross-section

Evolution of the parent population across the collision cell:

$$\begin{cases} \dfrac{dI_n(E)}{dt} = -<W_{n+1}>I_n(E) \\ \dfrac{dI_n(E')}{dt} = W_{n+1}I_n(E) - W_n^T(E')I_n(E') \\ \vdots \\ \dfrac{dI_{n-i}(E^{i+1})}{dt} = W_{n-i+1}(E^i)I_{n-i+1}(E^i) - W_{n-i}^T(E^{i+1})I_{n-i}(E^{i+1}) \\ \vdots \\ \dfrac{dI_1(E^n)}{dt} = W_2(E^{n-1})I_2(E^{n-1}) \end{cases}$$

$$\begin{cases} W_{n+1} = \rho\sigma v & \text{: collision rate, E} \rightarrow \text{E'} \\ W_{n-i}^T(E^{i+1}) & \text{: Total evaporation rate } n\text{-}i \rightarrow n\text{-}i\text{-}1 \text{ at total internal energy } E^{i+1} \\ W_{n-i}(E^{i+1}) & \text{: differential evaporation rate at total internal energy } E^{i+1} = E^{i+2} + \varepsilon_i + E_{Py} \end{cases}$$

Theoretical fragmentation cross-section

Evolution of the parent population across the collision cell:

$$I_n(E) = I_{0n} e^{-\langle W_{n+1} \rangle t}$$

$$I_{n-i}(E^{i+1}) = I_{0n} \prod_{j=-1}^{i-1} W_{n-j}(E^{j+1}) \sum_{j=-1}^{i} \frac{e^{-W_{n-j}^{T}(E^{j+1})}}{\prod_{\substack{k=-1 \\ k \neq j}}^{i} (W_{n-k}^{T}(E^{k+1}) - W_{n-j}^{T}(E^{j+1}))}$$

$$I_0 = \sum_i \sum_{E,J} \int dv \int db \prod_{j=1}^{i} \int_{E+Ec-\sum \varepsilon_j - \sum D_i = E^{i+1}} d\varepsilon_j \quad I_{n-i}(E^{i+1})$$

$$I = I_{0n} e^{-W_{n+1} t} + \sum_{E,J} \int dv \int db I_n(E')$$

Theoretical cross-section

After the collision cell, propagation during t_D :

$$I = \sum_E I_n(E) + \sum_E \sum_{E'} I_n(E') e^{-W(E')t_D}$$

$$\sum_{E'} = \int dv \int db\, f(v) P(b)$$

$$P(b) = \frac{2b}{(r+R)^2}$$

$$f(v) = \sqrt{\frac{2m}{\pi k_B T_{cel}}} \frac{v}{v_{ag}} e^{-\frac{m}{2k_B T_{cel}}(v_{ag}^2 + v^2)} \sinh\left(\frac{m v_{ag} v}{k_B T_{cel}}\right)$$

Evaporation of pyrene clusters

- Reminder of the experiment:

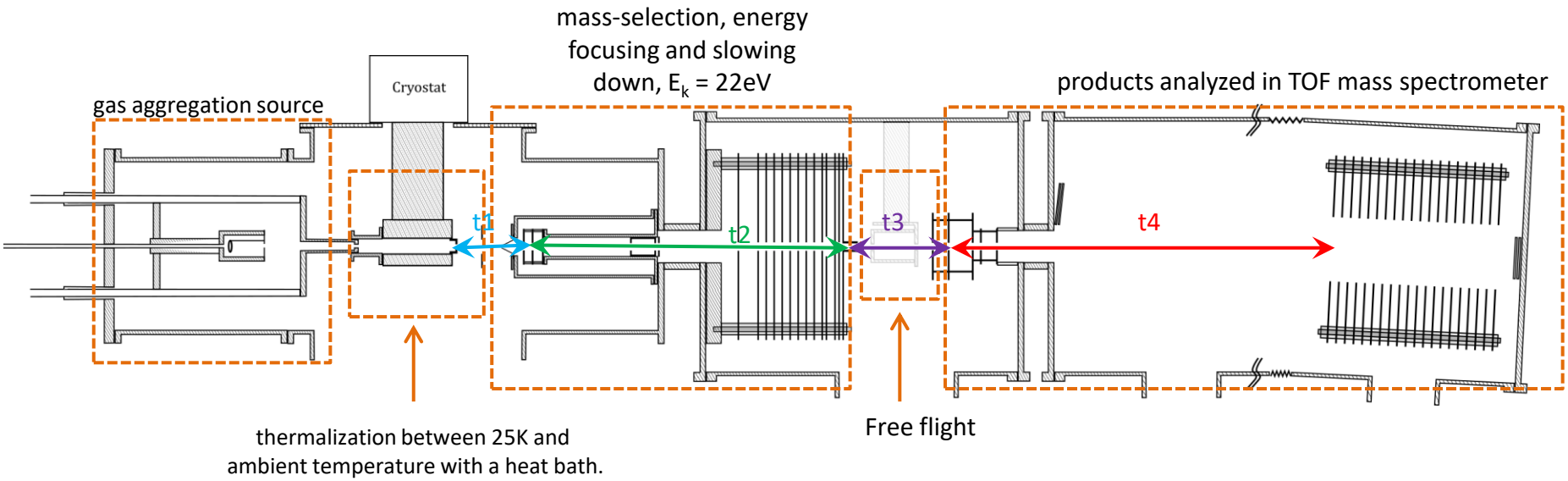

Goal of the experiment: determine the temperature dependant evaporation rate W(T) for each sizes.

Example: $(Py)_{11}^{+}$ @ 22 eV

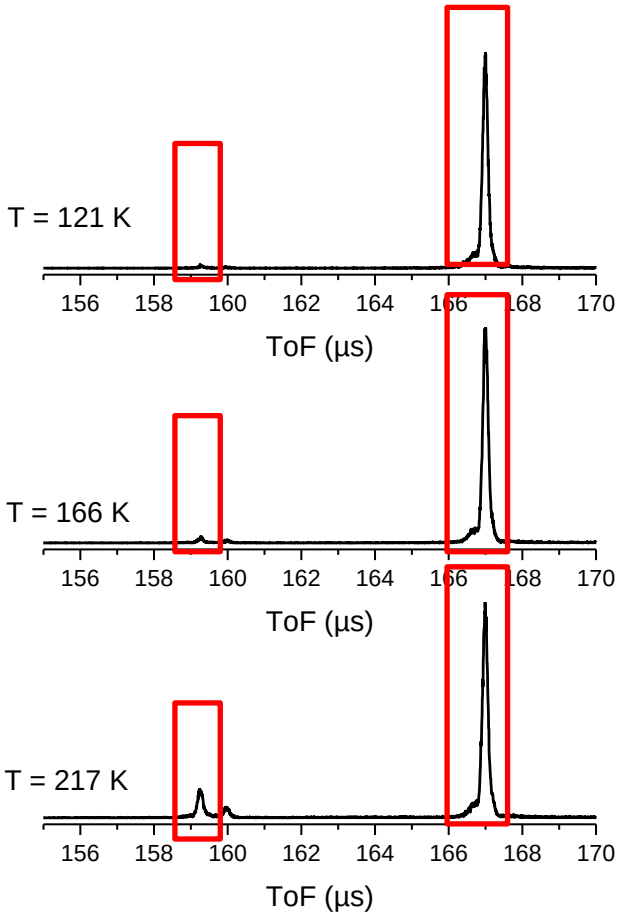

Evolution of the mass spectra of mass selected clusters with initial temperature.
As the temperature is raised, appearance of fragments due to evaporation

All spectra acquired in autumn 2016 reanalyzed:
-Gaussian fit of the peaks in the TOF
- Extraction of the ratio I/Io
I = parent peak intensity
Io = sum of parent + fragment peaks

At the thermalizer exit, each cluster size has a population $I_n^0(E,J)$ with an internal energy E and a total angular momentum J.

After the propagation time t1, the population of size n is:

$$I_n^1 = I_n^0 e^{-W_n(E,J)t_1} + I_{n+1}^0 (1 - e^{-W_{n+1}(E,J)t_1})$$

After acceleration by the first Wiley-McLaren up to the end of the slowing down/mass selection, if clusters evaporate they are discarded.

So after the propagation time t2, the population of size n becomes:

$$I_n^2 = I_n^0 e^{-W_n(E,J)(t_1+t_2)} + I_{n+1}^0 (1 - e^{-W_{n+1}(E,J)t_1})$$

Finally, after the free flight propagation time t3, we have:

$$I_n^3 = I_n^0 e^{-W_n(E,J)(t_1+t_2+t_3)} + I_{n+1}^0 (1 - e^{-W_{n+1}(E,J)t_1})$$

Nb: in what precedes, we assume that after one evaporation, clusters are cold enough so that no further evaporation occurs

If clusters evaporate after the second Wiley McLaren acceleration and before the reflectron (t4), they end up if the “secondary” fragment peak.

If they evaporate after the reflectron they can not be distinguished from the parent peak.

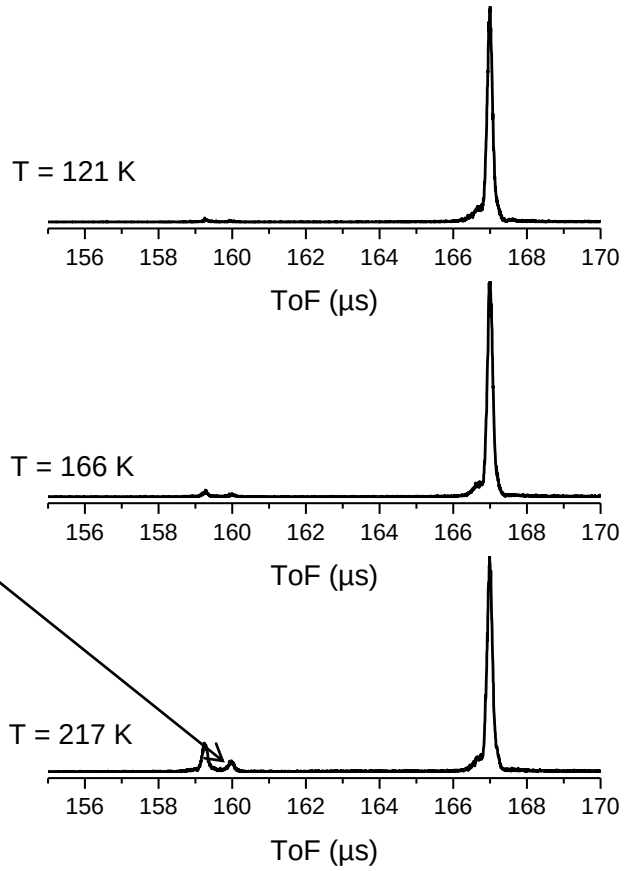

In the present analysis we consider only the intensity of the parent peak and of the fragment peak corresponding to evaporation in the free flight time t3.

The parent peak population in the TOF is therefore given by:

$$I_n^3 = I_n^0 e^{-W_n(E,J)(t_1+t_2+t_3+t_4)} + I_{n+1}^0 (1 - e^{-W_{n+1}(E,J)t_1})$$

And the fragment peak population in the TOF is :

$$I_{n-x}^3 = I_n^0 e^{-W_n(E,J)(t_1+t_2)} (1 - e^{-W_n(E,J)t_3})$$

The corresponding experimentally determined ratio is:

$$\frac{I_n^3}{I_n^3 + I_{n-x}^3} = \frac{I_n^0 e^{-W_n(E,J)(t_1+t_2+t_3+t_4)} + I_{n+1}^0 (1 - e^{-W_{n+1}(E,J)t_1})}{I_n^0 e^{-W_n(E,J)(t_1+t_2+t_3+t_4)} + I_{n+1}^0 (1 - e^{-W_{n+1}(E,J)t_1}) + I_n^0 e^{-W_n(E,J)(t_1+t_2)} (1 - e^{-W_n(E,J)t_3})}$$

Assuming $I_n^0 \approx I_{n+1}^0$ and $W_n(E,J) \approx W_{n+1}(E,J)$ it follows:

$$\frac{I_n^3}{I_n^3 + I_{n-x}^3} = \frac{1 - e^{-W(E,J)t_1} + e^{-W(E,J)(t_1+t_2+t_3+t_4)}}{1 - e^{-W(E,J)t_1} + e^{-W(E,J)(t_1+t_2)}}$$

For n = 10 @ 22 eV, we have:

t1 = *D/vo*
t2 = 76 μs
t3 = 78.5 μs
t4 = 74 μs

D = distance between the exit of the thermalizer and the first Wiley-McLaren = 8 cm

v_0 = thermal velocity of helium

So for a size *n*:

$$t1 = D / v_0$$

$$t2 = 76\sqrt{\frac{n}{10}}$$

$$t3 = 78.5\sqrt{\frac{n}{10}}$$

$$t3 = 74\sqrt{\frac{n}{10}}$$

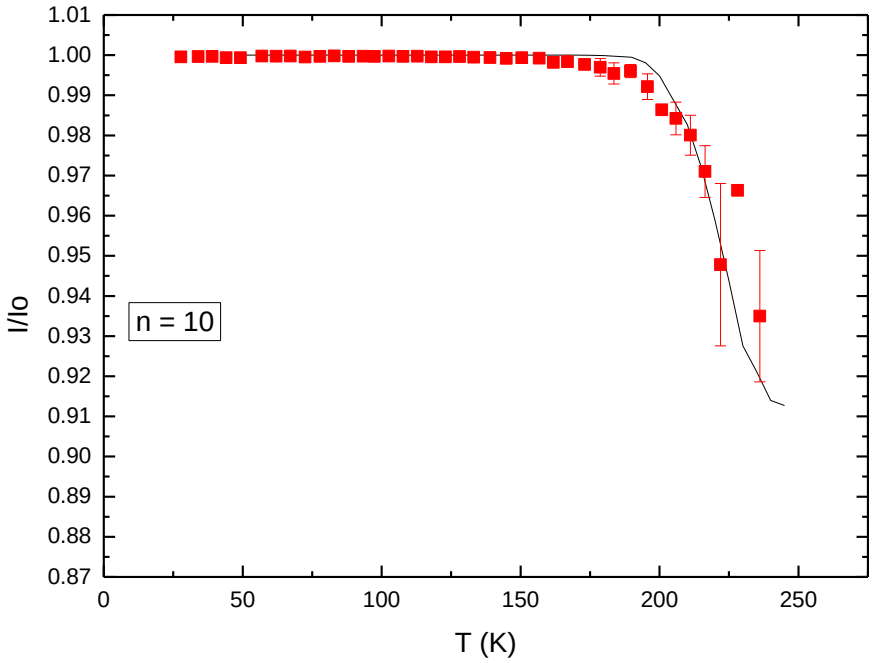

Example of experimentally determined ratio I/Io (red squares).
Black line = theory, description to follow.

Vibrational harmonic frequencies

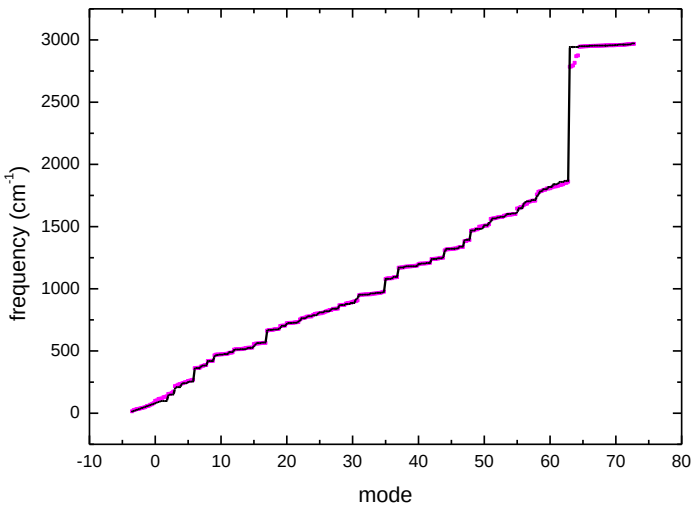

harmonic frequencies from Léo for the tetramer

Vibrational harmonic frequencies calculated for neutral pyrene and cationic clusters of sizes 1, 2, 3 and 4.

To extrapolate for larger sizes n:

Intramolecular frequencies = cation + (n-1) neutrals

Intermolecular frequencies = linear interpolation between 13 cm^{-1} and the lowest cationic frequency.

Vibrational harmonic frequencies and initial internal energy of the parent E(T)

Using these, the heat capacity of bulk pyrene can be reproduced:

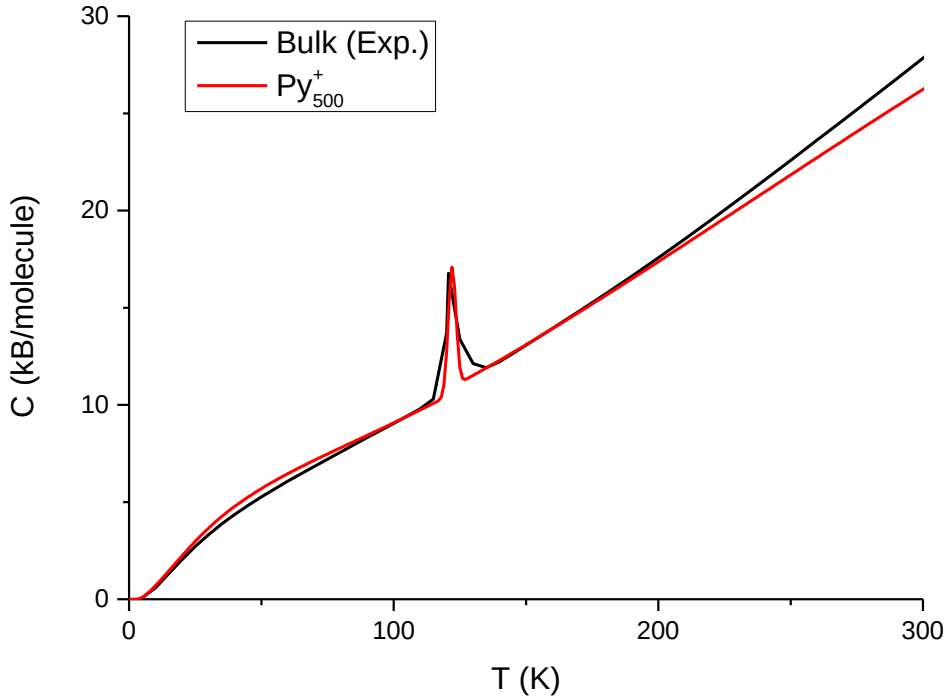

The phase transition around 120 K is accounted for by scaling the frequencies by 0.98 above 120 K.

The high temperature part remains poorly described.

Moments of inertia and rotational constants

For the PST calculation the rotational constant B is needed. $B = \frac{\hbar^2}{2I}$

The moment of inertia are taken as the geometrical average of the 3 main moments: $I = \sqrt[3]{I_1 I_2 I_3}$

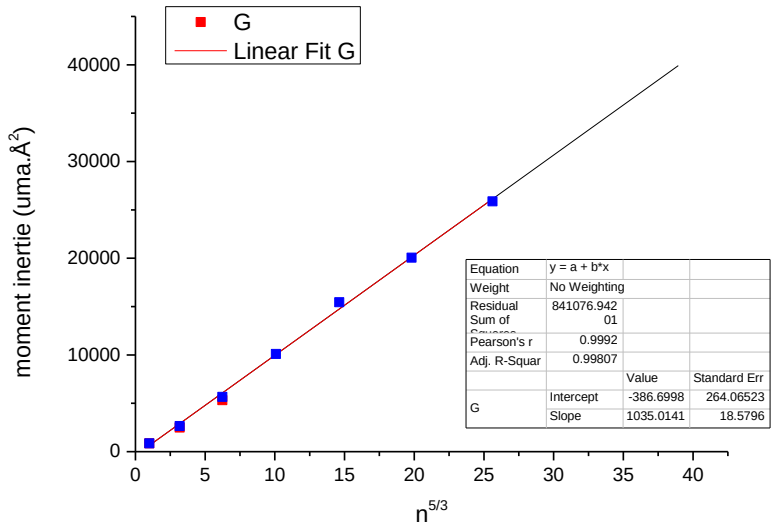

Squares: Léo's calculation

Line : $I(Py_n) \propto I(Py_1) n^{5/3}$

Monte Carlo integration

To compare with the experiment we need to calculate the quantity:

$$\frac{I_n^3}{I_n^3 + I_{n-x}^3} = \frac{\sum_J \int (1 - e^{-W(E,J)t_1} + e^{-W(E,J)(t_1+t_2+t_3)}) P(E,T) P(J,T) dE}{\sum_J \int (1 - e^{-W(E,J)t_1} + e^{-W(E,J)(t_1+t_2)}) P(E,T) P(J,T) dE}$$

P(E,T) = probability to have an internal energy E in the parent cluster.

Number occupation n_i of each vibration randomly picked up so that on average we have:

$$E = \sum_i \frac{\hbar\omega_i}{e^{\frac{\hbar\omega_i}{k_B T}} - 1}$$

P(J,T) = probability to have the total angular momentum J in the parent cluster.

$$P(J) = 2Je^{-\frac{BJ^2}{k_B T}}$$ High temperature or low B limit used

Monte Carlo integration

$$n_i = \mathrm{int}\left(-\frac{k_B T}{\hbar \omega_i} \ln(1-\xi) \right)$$

$$J = \mathrm{int}\left(-\sqrt{\frac{k_B T}{B} \ln(1-\xi)} \right)$$

ξ = uniform random variable

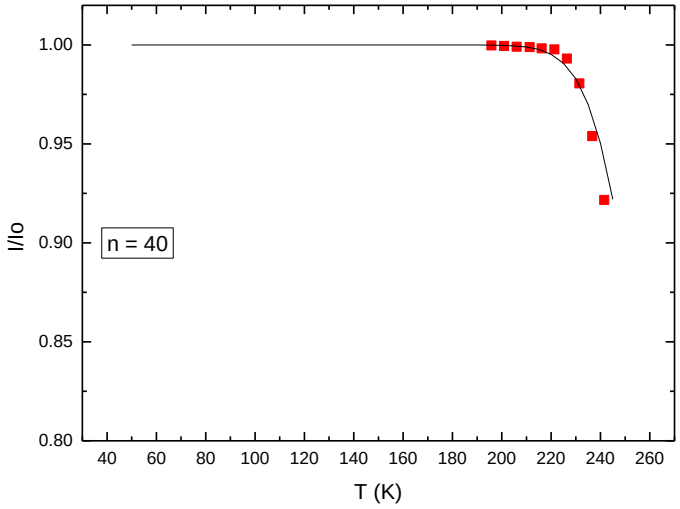
n = 40
I/Io
T (K)
1.00
0.95
0.90
0.85
0.80
40 60 80 100 120 140 160 180 200 220 240 260

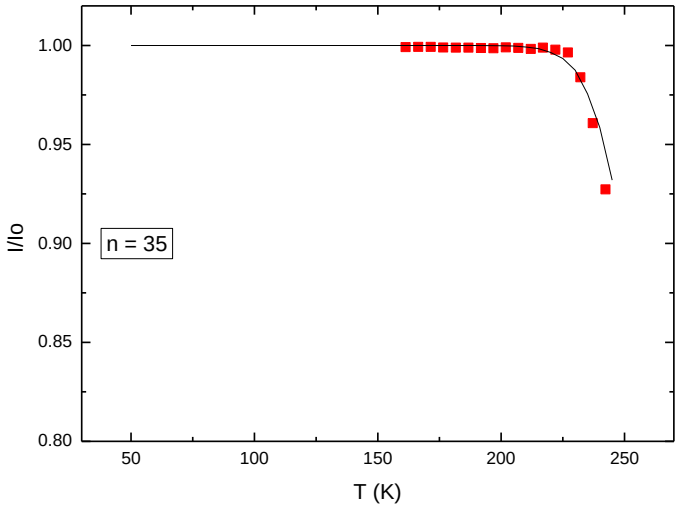
n = 35
I/Io
T (K)
1.00
0.95
0.90
0.85
0.80
50 100 150 200 250

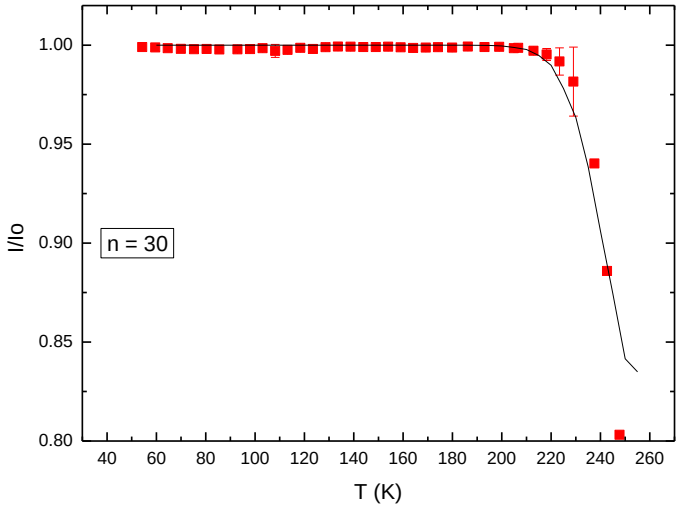
n = 30
I/Io
T (K)
1.00
0.95
0.90
0.85
0.80
40 60 80 100 120 140 160 180 200 220 240 260

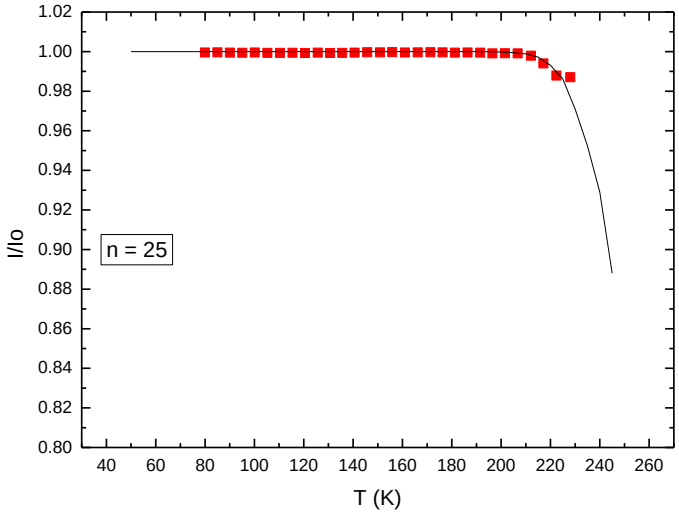
n = 25
I/Io
T (K)
1.02
1.00
0.98
0.96
0.94
0.92
0.90
0.88
0.86
0.84
0.82
0.80
40 60 80 100 120 140 160 180 200 220 240 260

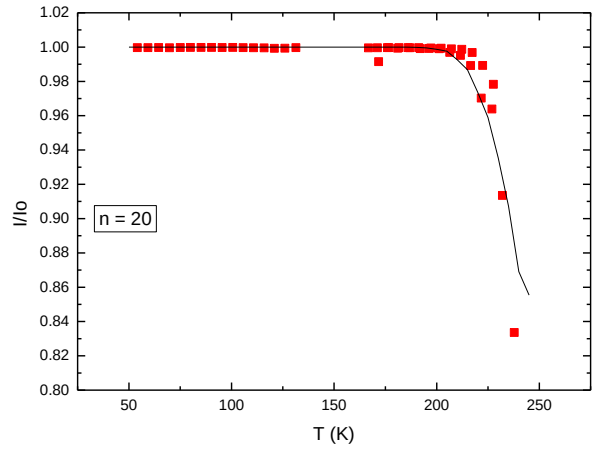
n = 20
I/Io
T (K)

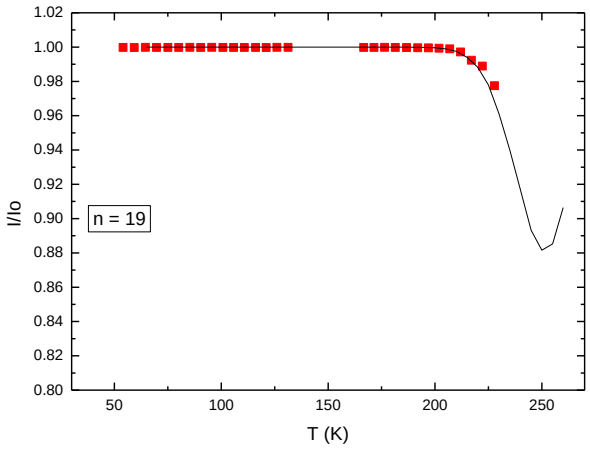
n = 19
I/Io
T (K)

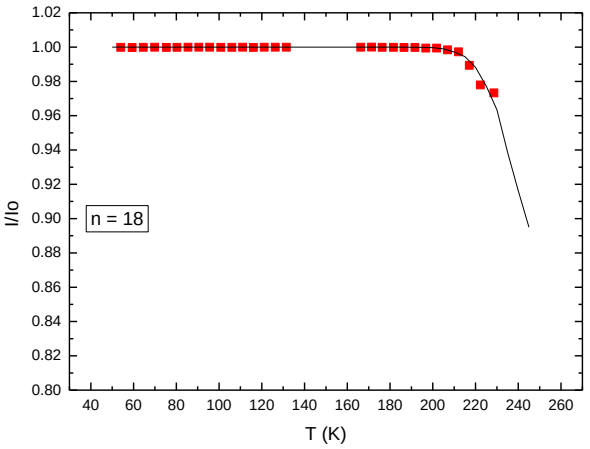
n = 18
I/Io
T (K)

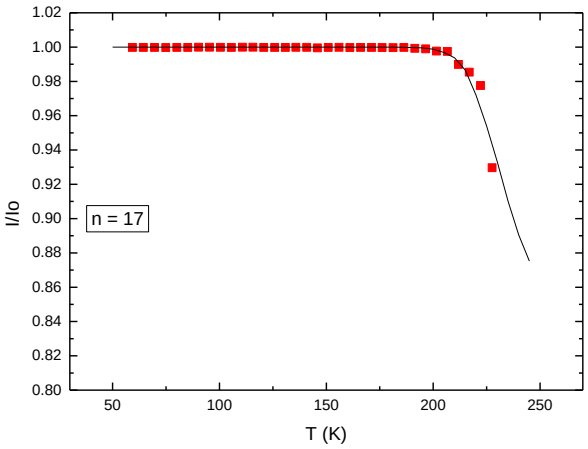
n = 17
I/Io
T (K)

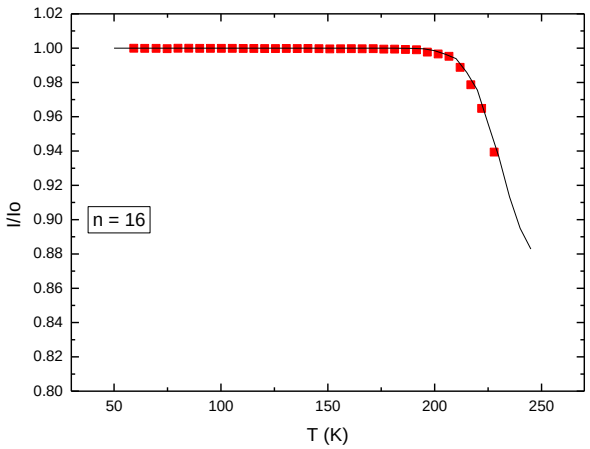
n = 16
I/Io
T (K)

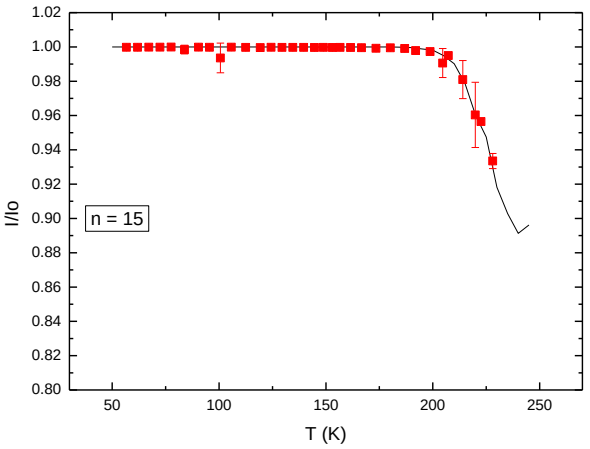
n = 15
I/Io
T (K)

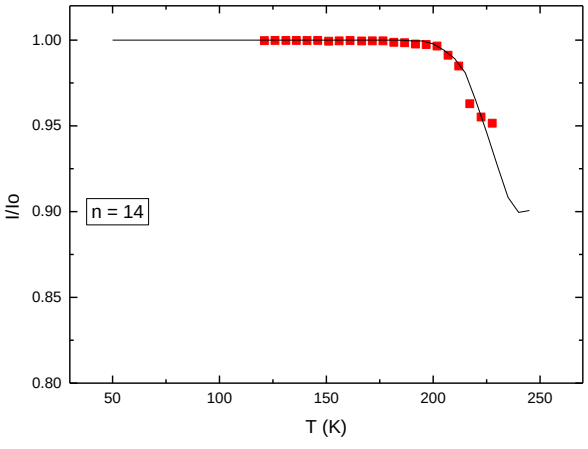
n = 14
I/Io
T (K)

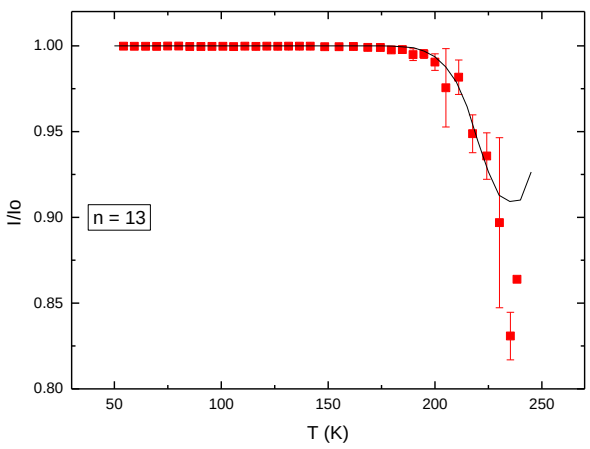
n = 13
I/Io
T (K)

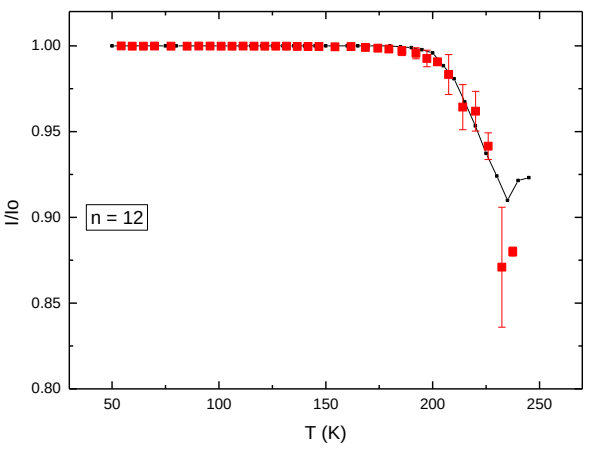
n = 12
I/Io
T (K)

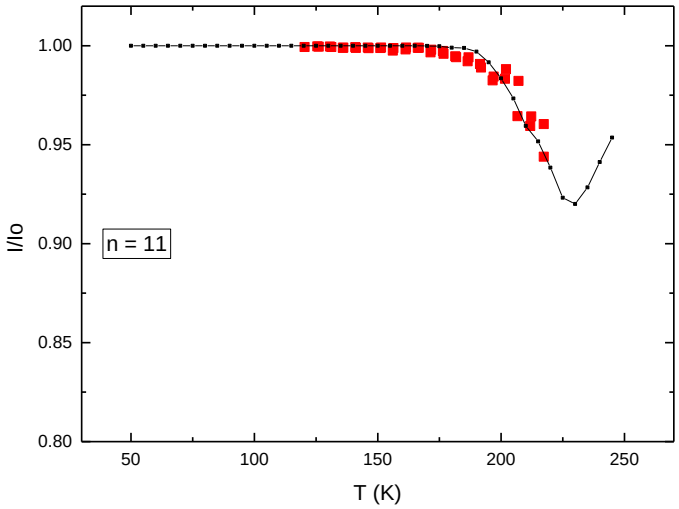
n = 11
I/Io
T (K)
1.00
0.95
0.90
0.85
0.80
50
100
150
200
250

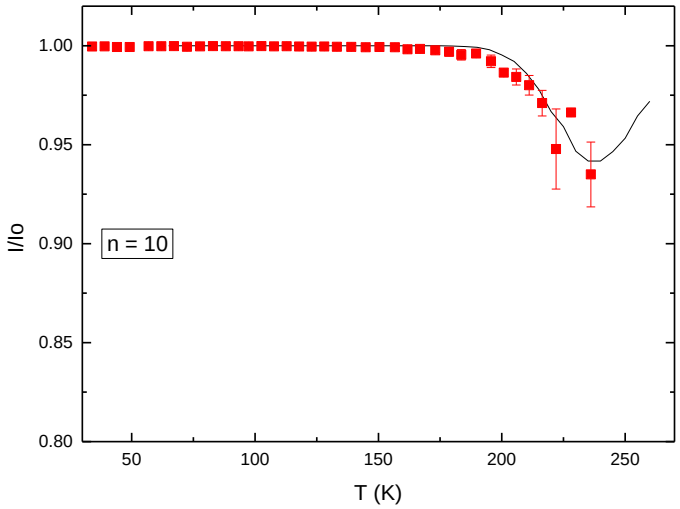
n = 10
I/Io
T (K)
1.00
0.95
0.90
0.85
0.80
50
100
150
200
250

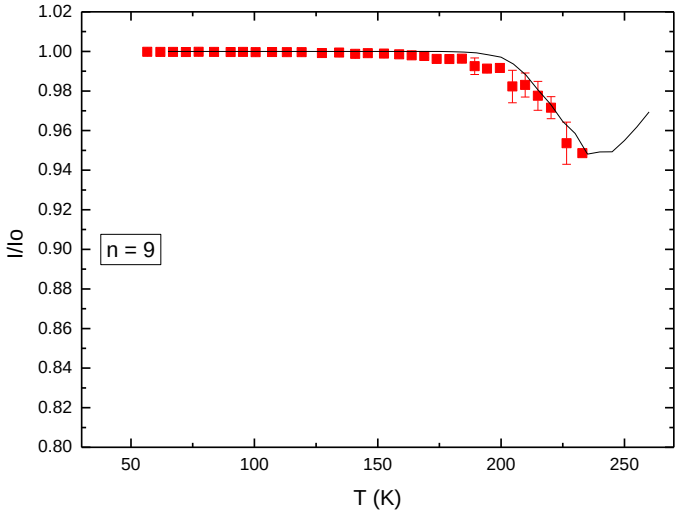
n = 9
I/Io
T (K)
1.02
1.00
0.98
0.96
0.94
0.92
0.90
0.88
0.86
0.84
0.82
0.80
50
100
150
200
250

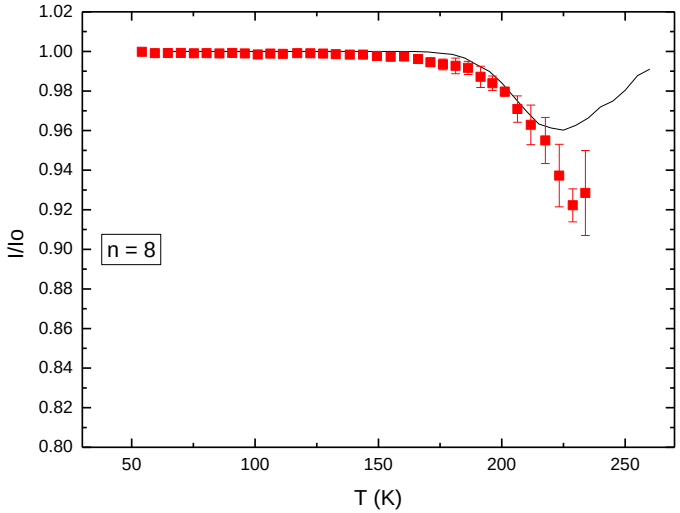
n = 8
I/Io
T (K)
1.02
1.00
0.98
0.96
0.94
0.92
0.90
0.88
0.86
0.84
0.82
0.80
50
100
150
200
250

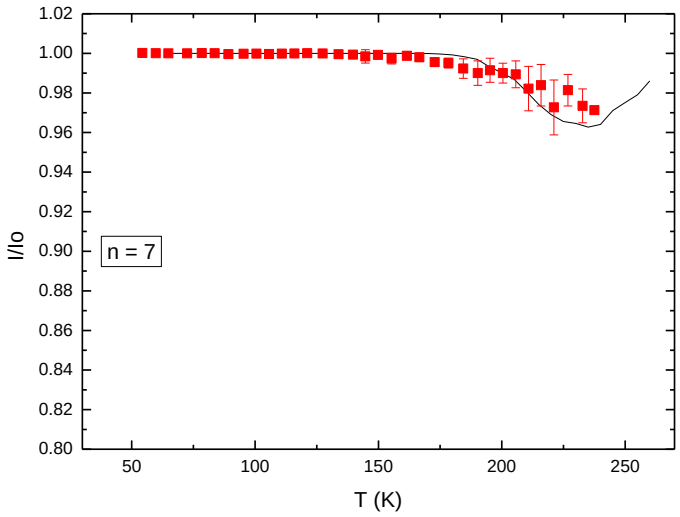
n = 7
I/Io
T (K)

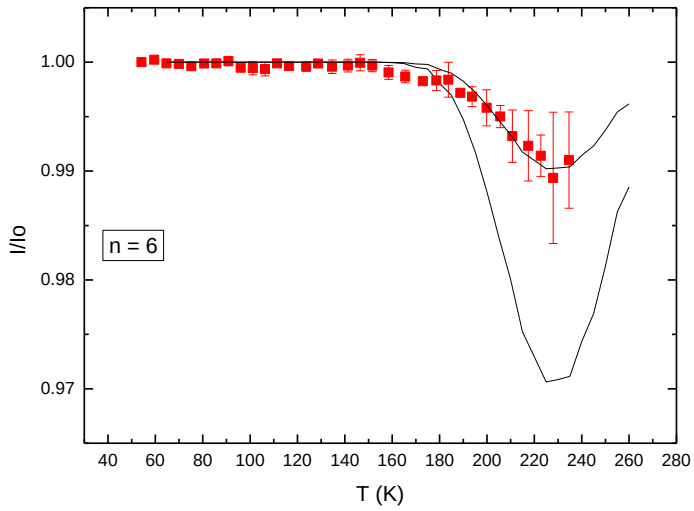
n = 6
I/Io
T (K)

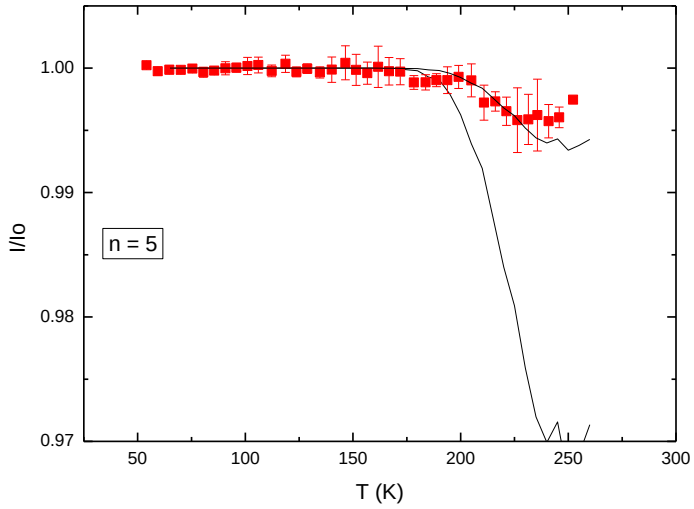
n = 5
I/Io
T (K)

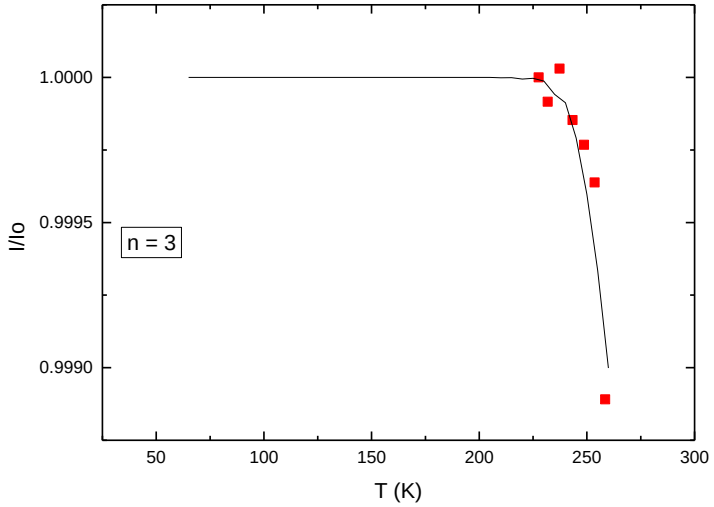
n = 3
I/Io
T (K)

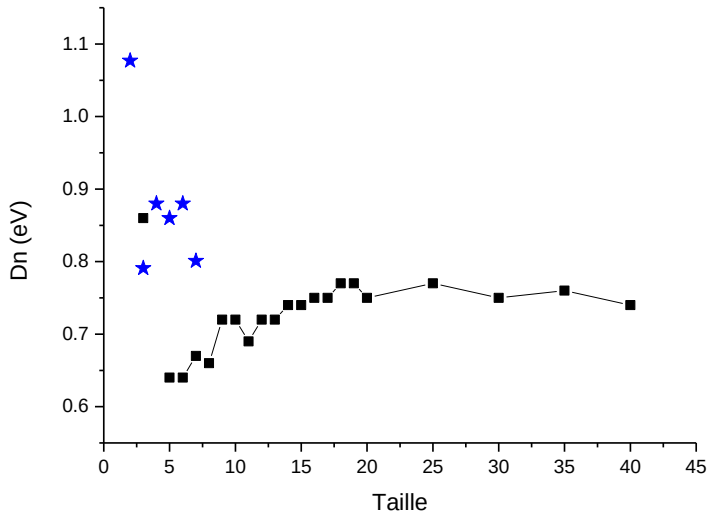

Blue stars: theory

Black squares: values deduced from the reproduction of the experimental curves using PST

n=3: to be confirmed, very low signal

n=5,6: scaling to reproduce the experimental data

Bulk: ΔH_{vap} ~ 0.94 eV @ 298 K

ΔH_{vap} ~ 0.78 eV @ 400 K